

Journal Pre-proof

The Quest of the Best – A SAR Study of Trithiolato-Bridged Dinuclear Ruthenium(II)-Arene Compounds Presenting Antiparasitic Properties

Emilia Păunescu, Ghalia Boubaker, Oksana Desiatkina, Nicoleta Anghel, Yosra Amdouni, Andrew Hemphill, Julien Furrer



PII: S0223-5234(21)00459-1

DOI: <https://doi.org/10.1016/j.ejmech.2021.113610>

Reference: EJMECH 113610

To appear in: *European Journal of Medicinal Chemistry*

Received Date: 8 April 2021

Revised Date: 18 May 2021

Accepted Date: 1 June 2021

Please cite this article as: E. Păunescu, G. Boubaker, O. Desiatkina, N. Anghel, Y. Amdouni, A. Hemphill, J. Furrer, The Quest of the Best – A SAR Study of Trithiolato-Bridged Dinuclear Ruthenium(II)-Arene Compounds Presenting Antiparasitic Properties, *European Journal of Medicinal Chemistry*, <https://doi.org/10.1016/j.ejmech.2021.113610>.

This is a PDF file of an article that has undergone enhancements after acceptance, such as the addition of a cover page and metadata, and formatting for readability, but it is not yet the definitive version of record. This version will undergo additional copyediting, typesetting and review before it is published in its final form, but we are providing this version to give early visibility of the article. Please note that, during the production process, errors may be discovered which could affect the content, and all legal disclaimers that apply to the journal pertain.

© 2021 Published by Elsevier Masson SAS.

The Quest of the Best – A SAR Study of Trithiolato-Bridged Dinuclear Ruthenium(II)-Arene Compounds Presenting Antiparasitic Properties

Emilia Păunescu,^{a,*} Ghalia Boubaker,^{b,||} Oksana Desiatkina,^a Nicoleta Anghel,^b Yosra Amdouni,^{b,c} Andrew Hemphill^{b,*} and Julien Furrer^{a,*}

^aDepartment of Chemistry, Biochemistry and Pharmaceutical Sciences, University of Bern, Freiestrasse 3, 3012 Bern, Switzerland.

^bInstitute of Parasitology, Vetsuisse Faculty, University of Bern, Länggass-Strasse 122, 3012 Bern, Switzerland.

^cLaboratoire de Parasitologie, Université de la Manouba, Institution de la Recherche et de l'Enseignement Supérieur Agricoles, École Nationale de Médecine Vétérinaire de Sidi Thabet, Sidi Thabet 2020, Tunisia.

^{||}equal contributions

Abstract

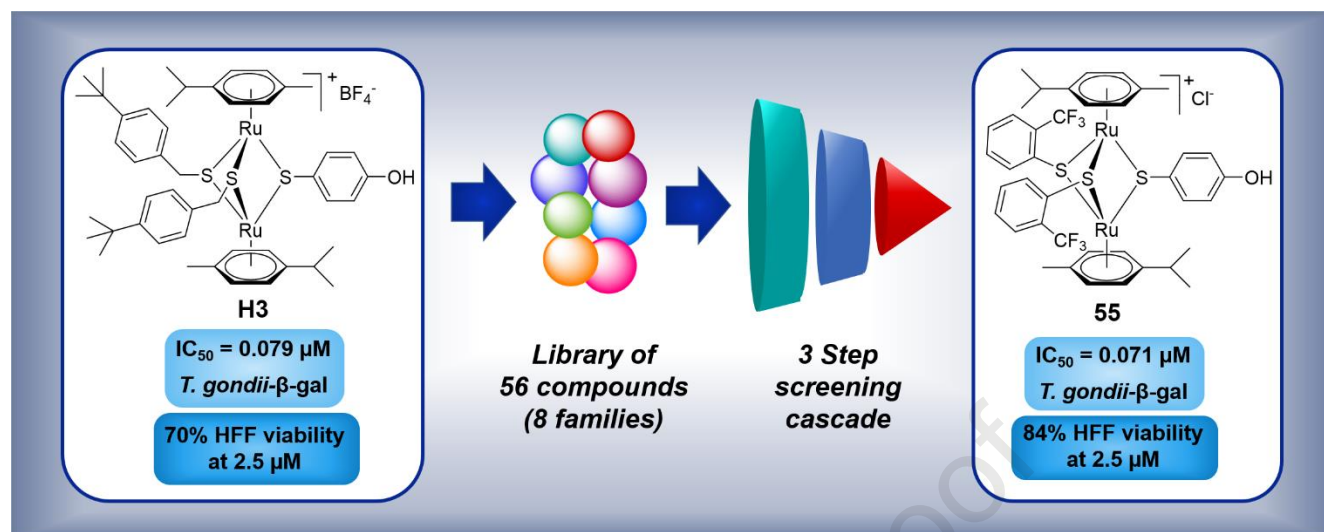
A structure activity relationship (SAR) study of a library of 56 compounds (54 ruthenium and 2 osmium derivatives) based on the trithiolato-bridged dinuclear ruthenium(II)-arene scaffold (general formula $[(\eta^6\text{-arene})_2\text{Ru}_2(\mu_2\text{-SR})_3]^+$, symmetric and $[(\eta^6\text{-arene})_2\text{Ru}_2(\mu_2\text{-SR}^1)_2(\mu_2\text{-SR}^2)]^+$, mixed, respectively) is reported. The 56 compounds (of which 34 are newly designed drug candidates) were synthesized by introducing chemical modifications at the level of bridge thiols, and they were grouped into eight families according to their structural features. The selected fittings were guided by previous results and focused on a fine-tuning of the physico-chemical and steric properties. Newly synthesized complexes were characterized by NMR spectroscopy, mass spectrometry and elemental analysis, and four single-crystal X-ray structures were obtained.

The *in vitro* biological assessment of the compounds was realized by applying a three-step screening cascade: (i) evaluation of the activity against *Toxoplasma gondii* RH strain tachyzoites expressing β -galactosidase (*T. gondii*- β -gal) grown in human foreskin fibroblast monolayers (HFF) and assessment of toxicity in non-infected HFF host cells; (ii) dose-response assays using selected compound, and (iii) studies on the effects in murine splenocytes.

A primary screening was performed at 1 and 0.1 μM , and resulted in the selection of 39 compounds that inhibited parasite proliferation at 1 μM by more than 95% and reduced the viability of HFF by less than 49%. In the secondary screening, dose-response assays showed that the selected compounds exhibited half maximal inhibitory concentration (IC_{50}) values for *T. gondii*- β -gal between 0.01 μM and 0.45 μM , with 30 compounds displaying an IC_{50} lower than 0.1 μM . When applied to non-infected HFF monolayers at 2.5 μM , 8 compounds caused more than 90% and 31 compounds more than 30% viability impairment. The tertiary screening included 14 compounds that did not cause HFF viability loss higher than 50% at 2.5 μM . These derivatives were assessed for potential immunosuppressive activities. First, splenocyte viability was assessed after treatment of cells with concanavalin A (ConA) and lipopolysaccharide (LPS) with compounds applied at 0.1 and 0.5 μM . Subsequently, the 5 compounds exhibiting the lowest splenocyte toxicity were further evaluated for their potential to inhibit B and T cell proliferation.

Overall, compound **55** $[(\eta^6\text{-}p\text{-MeC}_6\text{H}_4\text{Pr}^i)_2\text{Ru}_2(\mu_2\text{-SC}_6\text{H}_4\text{-}o\text{-CF}_3)_2(\mu_2\text{-SC}_6\text{H}_4\text{-}p\text{-OH})]\text{Cl}$ exhibited the most favorable features, and will be investigated as a scaffold for further optimization in terms of anti-parasitic efficacy and drug-like properties.

Graphical abstract



Keywords: trithiolato-bridged dinuclear ruthenium(II)-arene compounds, *Toxoplasma gondii*, structure activity relationship study, antiparasitic activity, selectivity, human foreskin fibroblast viability, inhibition of immune cell proliferation.

1. Introduction

Despite the fact that parasites inflict widespread and important diseases in animals as well as in humans, drug development against parasitic diseases remains, with few exceptions, a largely neglected area. Many currently employed antiparasitic therapies exhibit important setbacks, such as adverse side effects and low efficacy, and the occurrence of resistance is being recognized as a serious constraint [1]. Consequently, the development of novel compounds is highly needed.

Toxoplasma gondii (*T. gondii*), a member of the phylum Apicomplexa, is an obligate intracellular protozoan that infects most mammalian species [2,3] and birds [4]. *Toxoplasma* has a high zoonotic potential, and it is estimated that up to 30% of the human population is infected [5,6]. However, serious disease affects only a fraction of infected persons. For example, primary infection during pregnancy can cause congenital toxoplasmosis [7,8], and foetal infection may lead to severe complications, including spontaneous miscarriage and malformations such as hydrocephalus, developmental retardation, and ocular toxoplasmosis causing eyesight impairment and even blindness in later life [9,10]. Likewise, reactivated toxoplasmosis, or acquisition of a primary infection, in immunocompromised patients will lead to acute toxoplasmosis, multiple organ failure and possibly death [11,12]. Most importantly, *T. gondii* is a major economic burden for the food industry, in that it affects food safety and food security by infecting most farm animal species used in food production [13].

The most frequently applied treatments for toxoplasmosis rely mainly on the use of a combination of pyrimethamine and sulfadiazine, supplemented with folinic acid to alleviate folic acid deficiency in the host [14]. Additional treatment options include trimethoprim/sulfamethoxazole, clindamycin, spiramycin and atovaquone [14]. Nevertheless, these drugs were initially developed for other diseases [15-18], and they are either of moderate efficacy and/or are prone to adverse side effects. Additionally, the current treatments target only tachyzoites, the rapidly replicating stage, while the latent bradyzoite cyst stage remains unaffected [2]. The increasing number of reports on treatment failures suggests that drug resistant strains are emerging [19]. Concluding, there is an urgent need for new, safe, low-cost and efficacious treatments against *T. gondii*.

Organometallic compounds could potentially provide interesting alternatives to current treatment options [20-26]. Following the pathway opened by cisplatin, important attention was given to the development of various metalorganic derivatives as prospective anticancer agents [27-35]. Among other ruthenium-based complexes, trithiolato-bridged dinuclear ruthenium(II)-arene compounds have shown high cytotoxicity against various cancer cell lines, as well as promising *in vivo* activity when assessed in tumor mouse models [36]. Besides anticancer activity, numerous metal-based compounds also display considerable antiparasitic properties [23,24,37-40].

Recent studies have shown promising anti-*Toxoplasma* activities of various metal-based compounds [41-52]. For example auranofin (**A**, Figure 1), a gold(I)-based complex approved for rheumatoid arthritis treatment, was shown to have a broad-spectrum antiparasitic activity against protozoan parasites [53] and to be effective against acute toxoplasmosis *in vitro* and *in vivo* [41].

Various coordination complexes of first row transition metal ions were shown to be active against the highly virulent *T. gondii* RH strain, with low cytotoxicity for non-infected mammalian cells, e.g., iron(III) complex **B** (Figure 1) [42], and a cobalt(II) complex [43] presenting similar organic ligands. Other compounds active against *Toxoplasma* include mononuclear copper(II) complexes **C1** and **C2** [44], with different naphthyl substituents (Figure 1).

Coordination complexes of zinc(II) [45] or iron(III) [46] (Figure 1, **D**) with sulfadiazine (drug used in combination with pyrimethamine for the treatment of toxoplasmosis) [14,15] exhibited better activity against *T. gondii* RH tachyzoites *in vitro* and lower host cell toxicity compared to sulfadiazine alone.

Compounds **E1/E2** [47] and **F** [48] (Figure 1) comprise covalently linked ferrocenyl moieties to bioactive ligands based on thiazolidinone units or atovaquone, and are efficient against *Toxoplasma* [54,55]. SAR (structure activity relationship) studies demonstrated that small modifications of the bioactive ligand were associated with important changes in antiparasitic activity and general cytotoxicity. For instance, ferrocenyl aminohydrohynaphthoquinone derivatives (Figure 1, **F**) presented a slightly lower activity compared to atovaquone against the atovaquone sensitive *T. gondii* PLK strain, but an improved activity against the atovaquone resistant ATO strain. Only compounds

presenting a certain length of the hydrophobic chain, and thus an associated lipophilicity, exhibited interesting antiparasitic activity, without exerting cytotoxicity in HFF (human foreskin fibroblast).

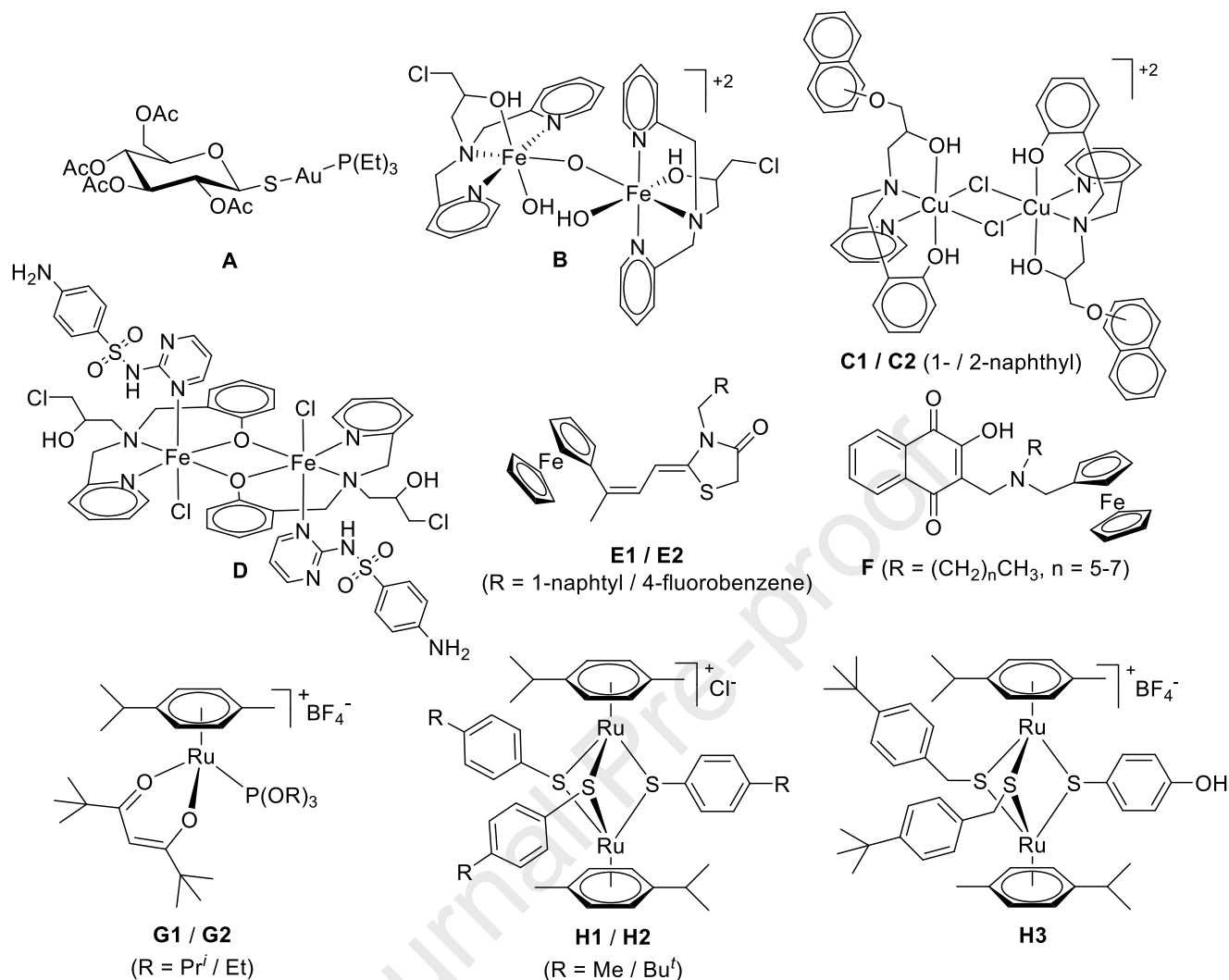


Figure 1. Structures of various metal complexes presenting anti-*Toxoplasma gondii* activity.

A range of hydrolytically stable half-sandwich η^6 -arene ruthenium(II) phosphite compounds [49,56] were previously evaluated for their *in vitro* activities against protozoan parasites such as *T. gondii* and the closely related *Neospora caninum*, and the helminth *Echinococcus multilocularis*. Results on *T. gondii* and *N. caninum* demonstrated that two compounds, namely **G1** and **G2** (Figure 1) exhibited a highly selective inhibitory effect on *in vitro* proliferation of tachyzoites without harming host cells. These findings prompted to further biological activity assessment of a small library of trithiolato-bridged dinuclear ruthenium(II)-arene complexes against protozoan parasites including *T. gondii* [50], *N. caninum* [57] and *Trypanosoma brucei* [58]. Three compounds **H1-H3** (Figure 1) were highly active against *T. gondii* with IC_{50} values (half maximal inhibitory concentrations) in low nanomolar range (34, 62 and 1.4 nM, respectively). Moreover, the viability of human foreskin fibroblast cells (HFF used as host cells) was not affected subsequent to incubation with high doses of complex **H1** or **H2** (~200 μM), whereas **H3** started to compromise HFF survival of at ~5 μM . In contrast to the *in*

vitro efficacy assessment data, compounds **H1-H3** were shown to be ineffective in the neosporosis mouse model at a dosage of $10 \text{ mg}\cdot\text{kg}^{-1}\cdot\text{day}^{-1}$) for 5 days [57].

Metallodrugs present a high potential not only as anticancer but also as antimicrobial, antiviral and antiparasitic agents [21,24,25,59]. Recent studies in medicinal inorganic chemistry aimed to extrapolate and adapt strategies that are well-established in organic drug discovery. This includes for example, the design of new compounds by employing fragment-based approaches [60,61] and pharmacophore conjugation strategy [62], the use of combinatorial coordination chemistry to access and study larger libraries of compounds [63,64], as well as the use of high-throughput screening assays [65,66]. Also, in the perspective of applying medicinal-chemistry approaches to metal-based bioactive compounds, an increasing number of reports focus on the development of series of compounds with the identification of descriptors and structure-activity relationships [67-72].

The limitations observed *in vivo* for compounds **H1-H3** [50,57,58] highlighted the necessity to identify thiolato-bridged dinuclear ruthenium(II)-arene compounds with improved properties as antiparasitic agents and to understand the structural features influencing their efficacy. The structure of trithiolato complexes (hydrophobic capping arene ligands, strong thiol bridges and absence of labile ligands) make them particularly inert towards hydrolysis, and more generally, ligand substitution. A fine balance of compounds' polarity/hydrophobicity can be reached by finely adjusting the substituents present on the bridge thiols. Based on **H1-H3**, a library of 56 thiolato-bridged dinuclear ruthenium(II)-arene and osmium(II)-arene compounds was designed, comprising a systematic tuning of the nature, position and number of the substituents present on the thiol bridge ligands. According to their respective structural characteristics the compounds were organized into eight families. For the biological assessment of the 56 compounds, a sequence of consecutive screening steps was considered (Figure 4). In the primary screening, all compounds were assessed for activity against *T. gondii*- β -gal and non-infected HFF at 0.1 and 1 μM . Compounds exhibiting $\geq 95\%$ parasite proliferation inhibition and $\leq 49\%$ impairment of HFF viability at 1 μM were then selected for a secondary screening, which comprised dose-response experiments yielding IC_{50} values for *T. gondii*- β -gal proliferation and an assessment of viability impairment in HFF monolayers at 2.5 μM . Only the compounds that did not cause HFF viability loss with more than 50% were subjected to a tertiary screening on their inhibitory potential in murine splenocyte cultures stimulated with lipopolysaccharide (LPS) and concanavalin A (ConA) to determine their effects on B and T cells viability and proliferative responses, respectively.

2. Results and discussion

2.1. Chemistry

Eight families of compounds based on the trithiolato-bridged dinuclear ruthenium(II)-arene scaffold were designed by applying a systematic approach. Various substituents were introduced at different

positions of the thiols' aromatic ring, for tuning their physico-chemical properties (polarity, hydrophobicity, ability to participate in H-bonding interactions). Detailed synthesis procedures and analysis of the new compounds are given in the *Supporting information*. An overview of the 56 compounds investigated in this study is presented Figure 2.

Journal Pre-proof

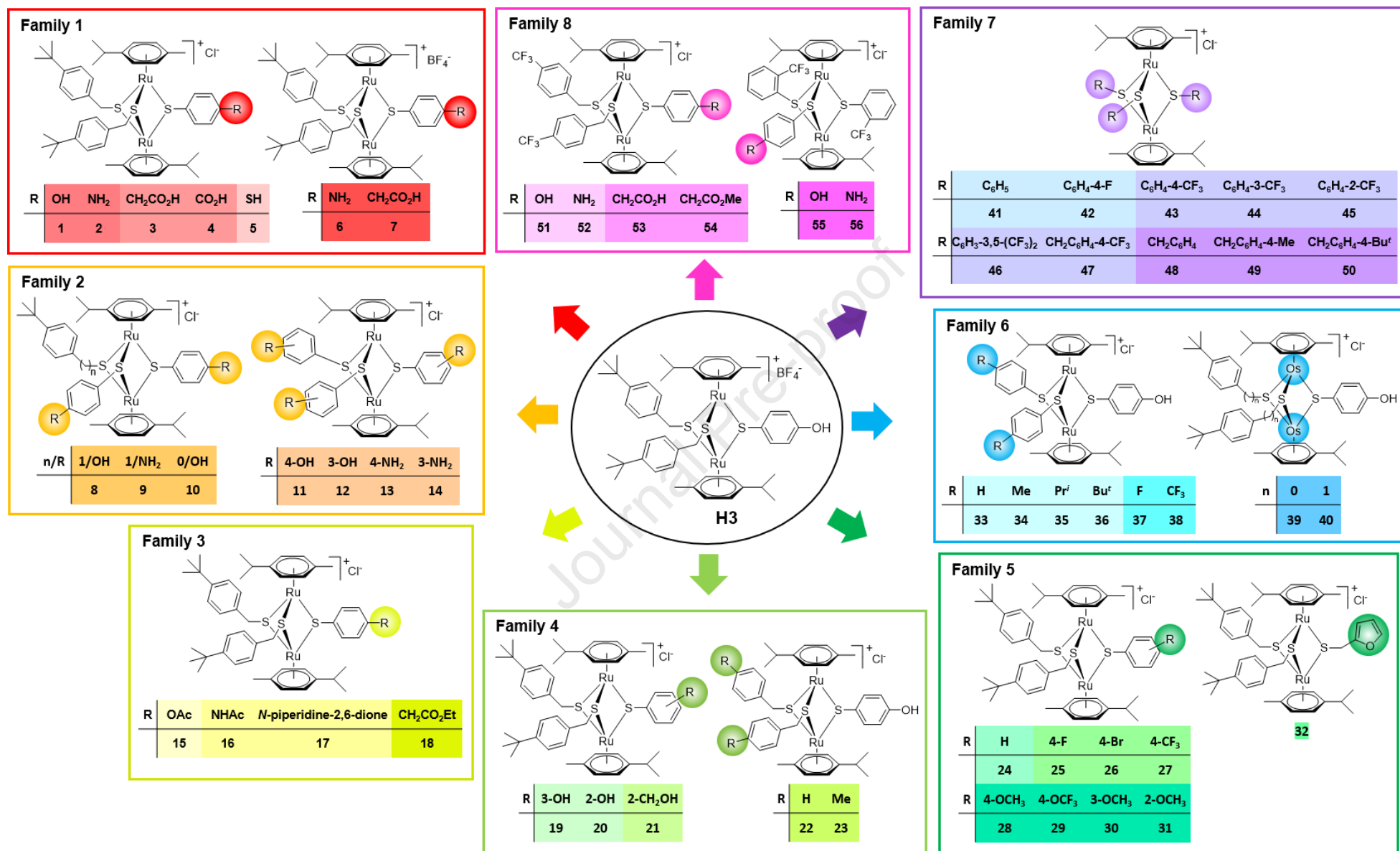
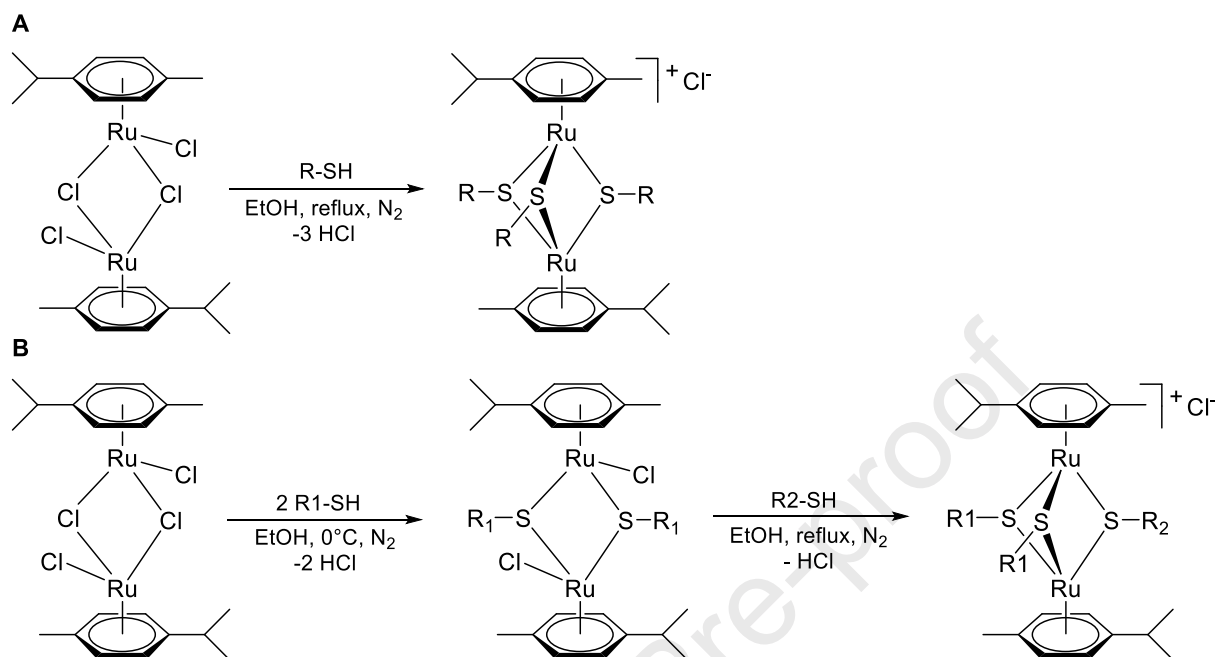


Figure 2. Structure of the 56 compounds investigated in this study organized in 8 families based on structural features modifications.

The symmetric trithiolato-bridged dinuclear ruthenium(II)-arene derivatives were obtained using adapted literature procedures [73-75] in one step as shown in Scheme 1A, starting from the ruthenium dimer $[\text{Ru}(\eta^6\text{-}p\text{-MeC}_6\text{H}_4\text{Pr}^i)\text{Cl}_2]_2$ and excess of the corresponding thiol (general procedure **A** in *Supporting information*).



Scheme 1. Synthesis of the symmetric (A) and mixed (B) trithiolato-bridged dinuclear ruthenium (II)-arene complexes.

The mixed cationic compounds were prepared in two steps adapting previously described protocol [76] following the reaction sequence presented in Scheme 1B. The dithiolato intermediates isolated after the reaction of one equivalent of ruthenium dimer $[\text{Ru}(\eta^6\text{-}p\text{-MeC}_6\text{H}_4\text{Pr}^i)\text{Cl}_2]_2$ with two equivalents of a first type of thiol (R1-SH in Scheme 1B, see general procedure **B** and **C** in *Supporting information*) were further reacted with a second type of thiol (R2-SH in Scheme 1B) used in excess (general procedure **D** in *Supporting information*). Most of the reactions for obtaining the mixed trithiolato compounds from the dithiolato compounds were performed in EtOH. In some cases (e.g., carboxylate analogues **3**, **4** and **53**) a mixture of CH_2Cl_2 /acetone was used as solvent to avoid esterification side reaction favored by the acid produced during the reaction. For the synthesis of compound **23** the solvent was a mixture of CH_2Cl_2 /MeOH to increase the solubility of the dithiolato intermediate **P4**.

Compounds **15** and **17** were obtained from the respective hydroxy and amine functionalized ruthenium complexes **1** and **2** using reactions presented in Schemes S1 and S2 in *Supporting information*.

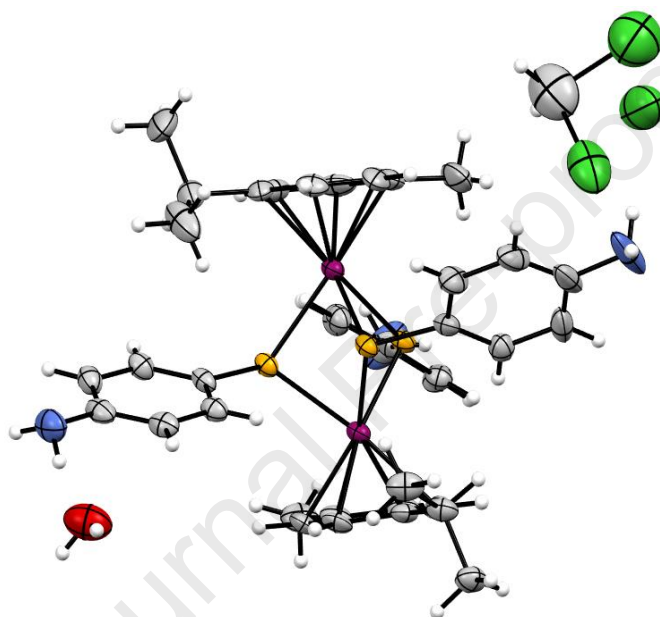
The new compounds were fully characterized by ^1H and ^{13}C NMR spectroscopy, mass spectrometry and elemental analysis. The representative peaks for the neutral dithiolato-bridged dinuclear ruthenium(II)-*p*-cymene (*p*-cymene : *p*-MeC₆H₄Pr^{*i*}) intermediates **P1-P13** correspond to $[\text{M-Cl}]^+$ ion,

due to the loss of a labile chlorine ligand. For the cationic trithiolato compounds **1-56**, the parent ion peak corresponds to the cation trithiolato di-ruthenium $[M-Cl]^+$ ion.

The compounds are readily soluble and stable in DMSO- d_6 which make them suitable for further biological tests (Figures S19-S27 in *Supporting information*).

The crystal structures of the symmetric complexes **13** and **43**, mixed complex **38** and dithiolato intermediate **P13** were established in the solid state by single-crystal X-ray diffraction (ORTEP representations shown in Figures 3 (A and B, S8 and S9), confirming the expected structure. Data collection and refinement parameters are given in Table S5 (*Supporting information*). Selected bond lengths and angles are presented in Tables S6, S7, S8 and S9.

A



B

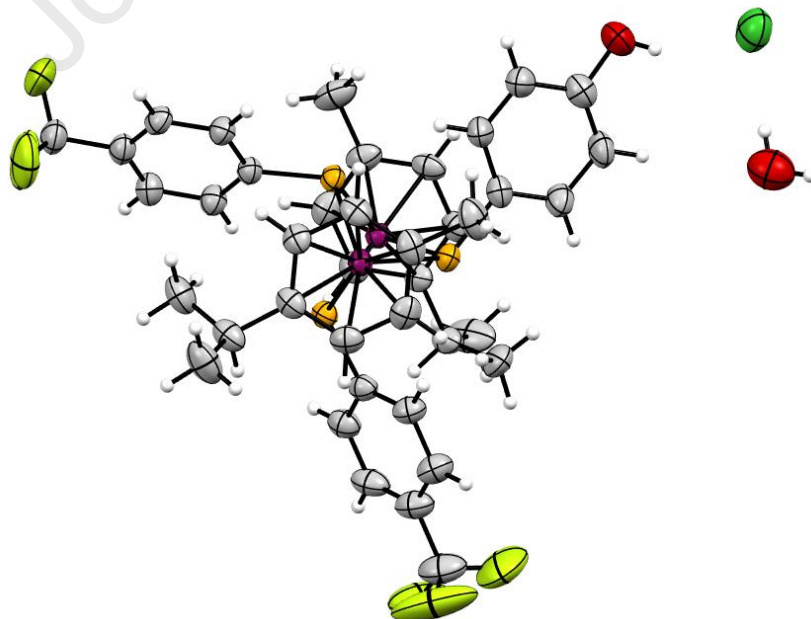


Figure 3. ORTEP representation of compounds **13** (A) and **38** (B) (thermal ellipsoids are 50% equiprobability envelopes, and H atoms are spheres of arbitrary diameter; the asymmetric unit of **13**

contains two independent complexes and two H₂O and two CH₂Cl₂ molecules, and the asymmetric unit of **38** contains one H₂O molecule).

Compounds **13** and **38** co-crystallize with solvent and H₂O molecules (**13**·CH₂Cl₂·H₂O and **38**·H₂O, Table S5). These solvent molecules not only fill the voids in the crystal packing, but also form a series of H-bonding interactions as presented in Figures S2 and S5 and Table S7 in *Supporting information*. In both structures, the ruthenium atoms adopt a pseudo-octahedral geometry with three sulphur atom ligands and the *p*-cymene ligand. In the case of the symmetric trithiolato compound **13**, both Ru(II) atoms adopt the typical piano-stool geometry with the *p*-cymene ligand being bound facially while the other three positions are occupied by three 4-aminothiophenolate ligands. The mixed **38** complex presents two 4-(trifluoromethyl) thiophenolate and one 4-hydroxythiophenolate as bridge thiols. To date, this is only the second example of an X-ray analysis of a mixed dinuclear trithiolato ruthenium(II)-arene complex [77]. The Ru₂S₃ unit forms a trigonal-bipyramidal framework; no metal-metal bonds are present, the corresponding distances being Ru(1)-Ru(2) 3.345 and Ru(3)-Ru(4) 3.346 for **13** (asymmetric unit contains two independent complexes) and Ru(1)-Ru(2) 3.347 Å for **38**. In both cations, the values of Ru–S bonds as well as the Ru–S–Ru angles (Table S6) are similar to those found in other symmetric or mixed *p*-cymene derivatives previously reported [74,77]. In both structures, the aromatic rings of the bridge thiols are tilted compared to the plane of the three sulphur atoms. Similar to the reported mixed complex **I** (Table S6) [77], the Ru-S-Ru and cent η^6 -cent(S-S-S)-cent η^6 angles in the mixed complex **38** show that the central di-ruthenium trithiolate unit is not symmetric. The presence of the two 4-(trifluoromethyl)thiophenolate ligands forces the dinuclear arene ruthenium unit to adopt a slightly distorted geometry, the planes of the two *p*-cymene ligands (C21–C26 and C31–C36) being tilted.

In the network of **13** is observed an interplay of H-bonding interactions involving both the chlorine anions and the H₂O molecules trapped in the crystal. A dimeric organization is mediated by four H-bonding interactions: two chlorine anions bridge two di-ruthenium units at the level of their respective two amino groups (Figure S2, *Supporting information*). The remaining amino group of each of the symmetric di-ruthenium complexes is involved in H-bonding interactions with an H₂O molecule. Thus, all three amino groups of the symmetric trithiolato di-nuclear ruthenium(II)-arene complex **13** are involved in intermolecular H-bonding interactions, two of them interact with two chlorine anions and lead to the formation of a dimer with another di-ruthenium unit, while the third NH₂ group interacts *via* H-bonds with the H₂O molecule present. In network, these intermolecular H-bonding interactions lead to further arrangements e.g., with the formation of parallel chains of di-ruthenium complexes (Figure S3). In the crystal of **13** an intermolecular H- π interaction (distance 3.404 Å) between a H-atom from the *p*-cymene *iso*-propyl group and the aromatic ring of one of the aminothiols was also identified (Figure S4).

In the crystal packing of **38**, a H-bonding interaction between the chlorine anion and OH group of the 4-hydroxythiophenolate unit (Figure S5, *Supporting information*) was acknowledged. The chlorine anion also interacts *via* H-bonds with two H₂O molecules trapped in the network. These cooperative H-bonding interactions mediated by chlorine anions and H₂O molecules lead to further dimeric organisation (Figure S5) and dictate network packing for example in antisense chains connected *via* a zipper of H-bonds (Figure S7, *Supporting information*). For **38** other short intermolecular contacts (2.675 and, respectively, 2.615 Å) were identified between the O atom of the phenol and a *p*-cymene H atom, and a H atom from the *p*-cymene methyl substituent of a neighbouring molecule (Figure S6). Experimental details regarding the X-ray structure determination for complexes **43** and **P13**, as well as the corresponding structural details are presented in Tables S5, S8 and S9, and Figures S8 and S9 in the *Supporting information*.

2.2. Biological assessment

2.2.1. Screening strategy

The 56 compounds considered for this study were organized in 8 families based on their structural features, and were subjected to a sequential biological screening as summarized in Figure 4. The antiparasitic activity (proliferation inhibition) was evaluated using *T. gondii*-β-gal grown in HFF host cell monolayers [50], and the cytotoxic effects were studied in non-infected HFF monolayers. The potential impact on T and B cell viability and proliferation was investigated using concanavalin A (ConA) and lipopolysaccharide (LPS)-stimulated murine splenocyte cultures [51].

The primary screening (Figure 4) of all 56 compounds against *T. gondii*-β-gal tachyzoites and HFF was carried out at 0.1 and 1 μM concentrations. These two concentrations were chosen for several reasons, such as: (i) potential solubility issues at the higher concentration, (ii) assessments for anti-parasitic or host cell activity cannot be done by testing only one concentration, (iii) the *T. gondii* IC₅₀ values of potentially interesting compounds would be in the range of 0.1 μM, and (iv) the 1 μM concentrations provides first indications on potential cytotoxic effects. Also, testing two concentrations initially opens options for selecting compounds for the next screening steps. When applied at 1 μM, the compounds that inhibited *T. gondii*-β-gal proliferation by at least 95% and did not impair HFF viability by more than 49% were subjected to the next step. In the secondary screening, the selected compounds were submitted to dose response studies to determine the IC₅₀ values, and potential cytotoxicity in HFF was assessed at 2.5 μM. The complexes exhibiting HFF cytotoxicity 50% or less were further subjected to a tertiary screening using murine splenocytes. For this, splenocyte cultures were subjected to treatments with LPS (to stimulate B cells) or ConA (to stimulate T cells), and the effects of the compounds at 0.1 and 0.5 μM concentrations on cellular viability were determined. These two concentrations were chosen because (i) most of the selected compounds (including the anti-

toxoplasma drug pyrimethamine) inhibit *T. gondii* in this concentration range, (ii) isolated and proliferating spleen cells are likely to be more susceptible to compound effects than HFF, and (iii) it is unlikely that higher drug concentrations will be obtained in tested animals. The ruthenium complexes that impaired T cell viability by less than 50% and B cell viability by less than 10% were further evaluated for their capacity to suppress ConA- and LPS-induced T and B cell proliferation.

Journal Pre-proof

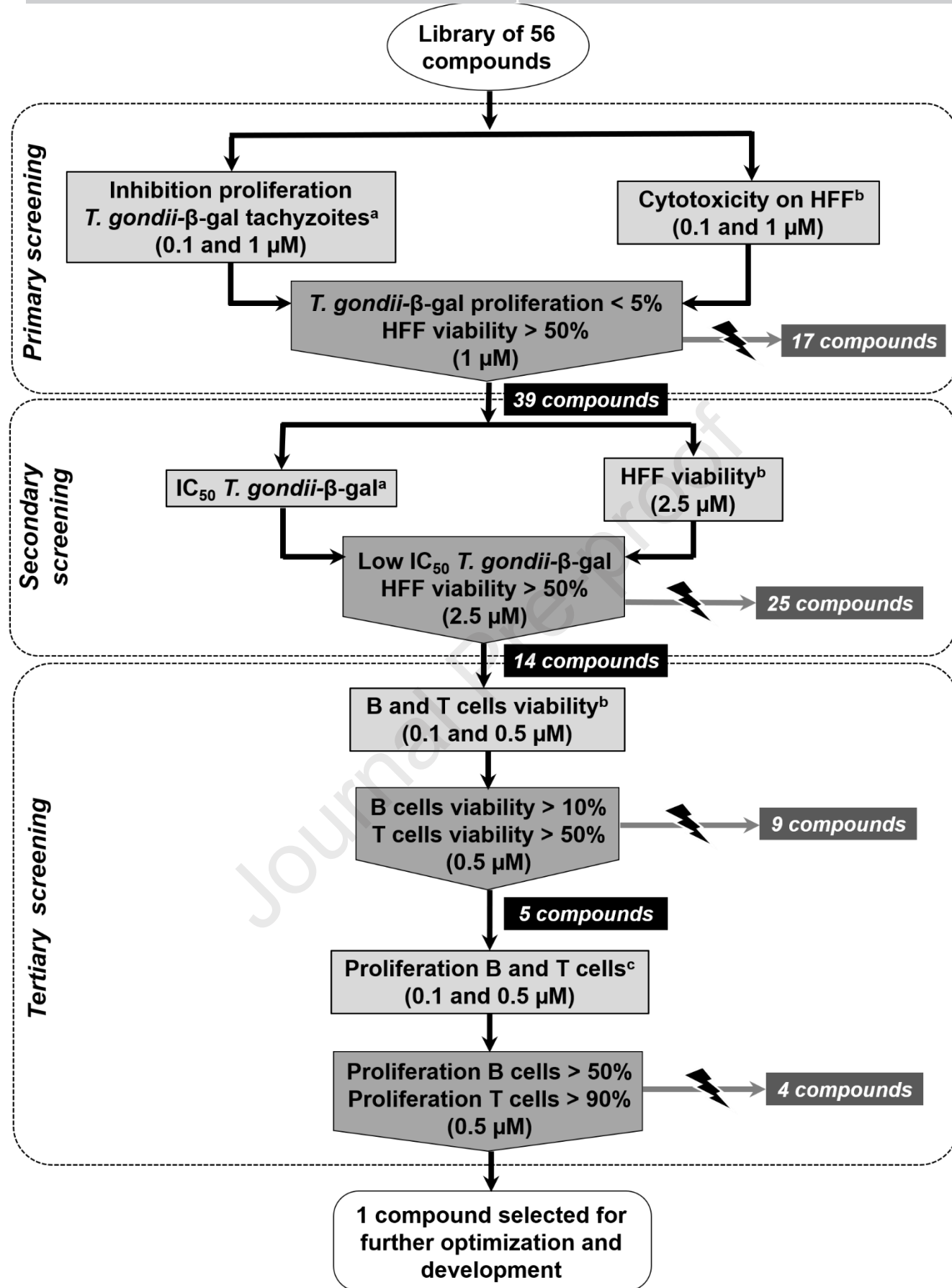


Figure 4. Schematic representation of the three-step screening cascade used for the assessment of the antiparasitic activity and cytotoxicity of the trithiolato-bridged dinuclear ruthenium(II)-arene

compounds. ^aβ-Galactosidase parasite proliferation assay. ^bAlamarBlue cell viability assay. ^cBrdU (5-bromo-2'-deoxyuridine) cell proliferations assay.

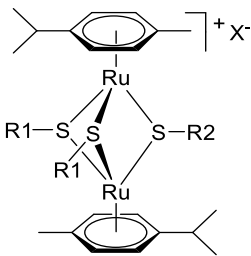
2.2.2. Primary screening

Detailed results of the primary screening are also provided in Table 5.

Family 1

Family 1 is comprised of 8 members whose structures are presented in Table 1, Figures 2 and S11. The BF₄⁻ salt of complex **H3** was previously shown to exhibit encouraging *in vitro* efficacy against *T. gondii*-β-gal tachyzoites [50] and it represents a lead compound for the design of other derivatives of the current study. For building the first series, the hydroxy group of **H3** was replaced by various polar groups: amino (**2**), thiol (**5**), and carboxy (**3** and **4**), the mixed compounds being synthesized as Cl⁻ salts. In order to assess the influence of the counterion on the biological activity, the series was completed with amino and carboxy compounds **6** and **7**, isolated as tetrafluoroborate (BF₄⁻) salts (Table 1).

Table 1. Structure of the compounds composing families 1 and 2.

	Compound	R1	R2	X ⁻
	H3 ^a	CH ₂ -C ₆ H ₄ -4-Bu ^t	C ₆ H ₄ -4-OH	BF ₄ ⁻
	Family 1			
	1 ^b	CH ₂ -C ₆ H ₄ -4-Bu ^t	C ₆ H ₄ -4-OH	Cl ⁻
	2	CH ₂ -C ₆ H ₄ -4-Bu ^t	C ₆ H ₄ -4-NH ₂	Cl ⁻
	3	CH ₂ -C ₆ H ₄ -4-Bu ^t	C ₆ H ₄ -4-CH ₂ -CO ₂ H	Cl ⁻
	4	CH ₂ -C ₆ H ₄ -4-Bu ^t	C ₆ H ₄ -4-CO ₂ H	Cl ⁻
	5	CH ₂ -C ₆ H ₄ -4-Bu ^t	C ₆ H ₄ -4-SH	Cl ⁻
	6	CH ₂ -C ₆ H ₄ -4-Bu ^t	C ₆ H ₄ -4-NH ₂	BF ₄ ⁻
	7	CH ₂ -C ₆ H ₄ -4-Bu ^t	C ₆ H ₄ -4-CH ₂ -CO ₂ H	BF ₄ ⁻
	Family 2			
	8 ^c	C ₆ H ₄ -4-OH	CH ₂ -C ₆ H ₄ -4-Bu ^t	Cl ⁻
	9	C ₆ H ₄ -4-NH ₂	CH ₂ -C ₆ H ₄ -4-Bu ^t	Cl ⁻
	10	C ₆ H ₄ -4-OH	C ₆ H ₄ -4-Bu ^t	Cl ⁻
	11 ^d	C ₆ H ₄ -4-OH	C ₆ H ₄ -4-OH	Cl ⁻
	12	C ₆ H ₄ -3-OH	C ₆ H ₄ -3-OH	Cl ⁻
	13	C ₆ H ₄ -4-NH ₂	C ₆ H ₄ -4-NH ₂	Cl ⁻
	14 ^e	C ₆ H ₄ -3-NH ₂	C ₆ H ₄ -3-NH ₂	Cl ⁻

^apreviously reported in ref. [50], ^bpreviously reported in ref. [76], ^dpreviously reported in ref. [50,74], ^epreviously reported in ref. [50,78].

The results of the primary screening at concentrations of 0.1 and 1 μM for family 1 are presented in Figures 5/6 and Table 5. Hydroxy functionalized compounds **H3** and **1**, with BF₄⁻ and Cl⁻ counterions, respectively, showed similar inhibition of parasite proliferation. Nevertheless, **1** did affect more than

H3 the viability of HFF for the same concentration. Amino derivative **6** with a BF_4^- counter-ion exhibited enhanced activity against *T. gondii* and less pronounced HFF toxicity compared to the corresponding Cl^- salt **2**. All carboxy derivatives tested, **3**, **4** and **7**, were toxic neither for *T. gondii* nor for HFF. The influence of the counterion (BF_4^- vs Cl^-) appeared less important than the nature of the polar substituent on one of the bridge thiols. The thiol functionalized compound **5**, more prone to oxidation, presented reduced activity against the parasite and less pronounced HFF toxicity compared to the hydroxy **1** and amino **2** analogues.

Family 2

Family 2 includes 7 compounds, for which the number (two mixed in complexes **8-10** and three in symmetric complexes **11-14**) and the position (*para* or *meta*) of the polar groups OH and NH_2 were systematically varied (Table 1, Figures 2 and S12). Compounds **11** and **14** were previously reported [74,78] and tested against *T. gondii*- β -gal under similar conditions [50].

The primary screening (Figures 5 and 6, Table 5) shows that compounds bearing two polar groups, namely **8** (hydroxy) and **9** (amino), were more toxic to both *T. gondii*- β -gal and HFF compared their analogues with a single polar substituent (**1** and **2**, respectively). The two compounds bearing three polar groups, **12** (hydroxy) and **13** (amino), were ineffective against both *T. gondii*- β -gal and HFF. These findings are supported by previous studies in which no activity was observed for compounds **11** and **14** [74,78]. The significantly increased toxicity in *T. gondii*- β -gal of **8** compared to **10** is interesting, as the structures of these compounds only differ by the presence of a methylene spacer in the bridge thiol bearing the Bu^t group. However, the effects of **8** and **10** on HFF viability were comparable, suggesting that the increased mobility of the bridge thiol bearing a Bu^t group could be beneficial for antiparasitic activity.

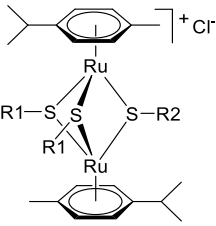
Overall, the data obtained for family 2 confirm previous findings [36] that the antiparasitic activity is influenced by the nature of the groups anchored on the bridged thiols, while the position of the substituents (*para* versus *meta*) has a lower influence.

Family 3

Family 3 comprises two esters (**15** and **18**) and two amides (**16** and **17**) derivatives from hydroxy amino and carboxy analogues **1**, **2** and **3** (Table 2, Figures 2 and S13). These structural modifications act as a protection of the polar groups preventing metabolic degradation (e.g., oxidation of the OH and NH_2 substituent to quinone or quinone-imine) or reaction/interaction with biomolecules. The proliferation of *T. gondii* tachyzoites was almost completely suppressed by **15-18** at 0.1 μM (Figure 5 and Table 5), whereas the polar parent analogues **1** and **2** displayed anti-*T. gondii*- β -gal activity only when applied at 1 μM , and **3** was completely inactive. Overall, compounds **15-18** are slightly more toxic for HFF than the more polar derivatives **1-3**. Modifying polar hydroxy (**1**), amino (**2**) or carboxy (**3**) groups into less

polar ester or amide substituents (**15-18**) enhanced significantly the potency against the parasite, and, to a lesser extent, the toxicity to HFF host cells.

Table 2. Structure of the compounds composing families 3 and 4.

	Compound	R1	R2
	Family 3		
	15	CH ₂ -C ₆ H ₄ -4-Bu ^t	C ₆ H ₄ - 4-OAc
	16	CH ₂ -C ₆ H ₄ -4-Bu ^t	C ₆ H ₄ - 4-NHAc
	17	CH ₂ -C ₆ H ₄ -4-Bu ^t	C ₆ H ₄ - 4-N-piperidine-2,6-dione
	18	CH ₂ -C ₆ H ₄ -4-Bu ^t	C ₆ H ₄ - 4-CH₂-CO₂Et
	Family 4		
	19	CH ₂ -C ₆ H ₄ -4-Bu ^t	C ₆ H ₄ - 3-OH
	20	CH ₂ -C ₆ H ₄ -4-Bu ^t	C ₆ H ₄ - 2-OH
	21	CH ₂ -C ₆ H ₄ -4-Bu ^t	C ₆ H ₄ - 2-CH₂OH
	22^a	CH ₂ -C ₆ H ₅	C ₆ H ₄ -4-OH
	23	CH ₂ -C ₆ H ₄ -4-Me	C ₆ H ₄ -4-OH

^apreviously reported in ref. [76] presenting BF₄⁻ as counterion.

Family 4

Family 4 includes 5 compounds, all containing a polar hydroxy group on one of the bridge thiols (Table 2, Figures 2 and S14). In this series, the influence of the OH group position (*meta* and *ortho*) in compounds **19** and **20**, was compared to that of *para*-analogue **1**. In derivative **21** the *ortho*-hydroxy group of **20** was replaced by a hydroxymethyl substituent, and in compound **23** the Bu^t substituents anchored on two of the bridged thiols in analogue **1** were replaced with less bulky and hydrophobic methyl substituents in the same *para* position. Compound **22** with an H atom as substituent had been previously reported [76] as BF₄⁻ salt and when tested against *T. gondii*-β-gal [50] was considered not interesting for further studies.

The primary screening (Figures 5 and 6 and Table 5) showed that *meta* and *ortho* hydroxy-substituted analogues **19** and **20**, were more efficient against *T. gondii* compared to the *para*-substituted compound **1**. A similar but stronger effect was observed for **21**, presenting a methylene spacer between the OH group and the aromatic ring, as well as for **23** bearing less bulky and hydrophobic Me substituents on two of the bridge thiols (compared to Bu^t in **1**). The position of the polar OH group present on one of the bridge thiols (**1**, **19** and **20**), but also the volume and lipophilicity of the substituents present on the other two thiols (**1** vs **23**) influence the parasite proliferation. The structural modifications in compounds **19-21** and **23** led to a decrease of host cell toxicity.

Family 5

Family 5 includes 9 members (Table 3, Figures 2 and S15). The role of the OH group in compound **1** was also questioned. In derivative **24** the hydroxy group was removed, whereas in compounds **25-27** it

was replaced by other polar substituents as fluoro, bromo or trifluoromethyl, respectively. Compared to **1**, in compounds **28** and **29** the *para*-OH group was protected as a methoxy and trifluoromethoxy ether. As the position of the OH group in **1** (*para*), **19** (*meta*) and **20** (*ortho*) influenced the antiparasitic efficacy, the effect of a methoxy group in the same positions was also established by comparing compounds **28** (*para*), **30** (*meta*) and **31** (*ortho*). The electron-rich *para*-phenoxy ring **1** was replaced in **32** with a methylene-furan-2-yl substituent.

Compared to **1**, the absence of the OH group in **24** increased both the anti-*Toxoplasma* efficacy and the viability of HFF (Figures 5 and 6 and Table 5). Likewise, the replacement of the hydroxy group in **1** with fluoro (**25**), bromo (**26**) and trifluoromethyl (**27**) polar substituents increased the antiparasitic activity and slightly reduced HFF toxicity. Both OH and F can participate in H-bonding interactions; nevertheless, while the OH group can be oxidized, this type of metabolization is less prone to take place if the position is blocked by fluoro, bromo or trifluoromethyl substituents.

Compounds **28** and **29** in which the hydroxy group in *para* position was protected as a methoxy or trifluoromethoxy group were more efficient against *T. gondii* and exhibited a lower HFF toxicity compared to **1**. *Meta* and *ortho* methoxy-substituted compounds **30** and **31** were similarly active against *T. gondii* as their respective hydroxy analogues **19** and **20**, but were significantly less toxic to HFF. Replacement of the *para*-phenoxy (**1**) with an electron rich furan ring in **32** also led to selective antiparasitic toxicity.

As previously observed for family 3, the results obtained for family 5 suggest that high efficacy against the parasite and reduced influence of the HFF viability are correlated with the presence of a polar group on one of the bridge thiols. Jointly, the presence of polar, chemically reactive groups, that can participate in H-bonding interactions (e.g., carboxyl) had a negative impact on the anti-*T. gondii* activity. Unreactive, polar substituents like fluoro (**25**), bromo (**26**), trifluoromethyl (**27**), methoxy (**28**, **30**, **31**) or trifluoromethoxy (**29**) answered these requirements and appeared to be better suited.

Regardless of the substituent position, all three methoxy derivatives **28**, **30** and **31** were highly efficient against *T. gondii*- β -gal when applied at 0.1 μ M. Some differences were observed in the effect on the HFF viability, for which *meta* and *ortho* substitution appeared to be more favorable.

Table 3. Structure of the compounds composing families 5 and 6.

Compound	R1	R2	M
Family 5			
24	CH ₂ -C ₆ H ₄ -4-Bu ^t	C ₆ H ₅	Ru
25	CH ₂ -C ₆ H ₄ -4-Bu ^t	C ₆ H ₄ -4-F	Ru
26	CH ₂ -C ₆ H ₄ -4-Bu ^t	C ₆ H ₄ -4-Br	Ru
27	CH ₂ -C ₆ H ₄ -4-Bu ^t	C ₆ H ₄ -4-CF ₃	Ru
28	CH ₂ -C ₆ H ₄ -4-Bu ^t	C ₆ H ₄ -4-OCH ₃	Ru
29	CH ₂ -C ₆ H ₄ -4-Bu ^t	C ₆ H ₄ -4-OCF ₃	Ru
30	CH ₂ -C ₆ H ₄ -4-Bu ^t	C ₆ H ₄ -3-OCH ₃	Ru

	31	CH ₂ -C ₆ H ₄ -4-Bu ^t	C ₆ H ₄ -2-OCH ₃	Ru
	32	CH ₂ -C ₆ H ₄ -4-Bu ^t	CH ₂ -furan-2-yl	Ru
	Family 6			
	33	C ₆ H ₅	C ₆ H ₄ -4-OH	Ru
	34	C ₆ H ₄ -4-Me	C ₆ H ₄ -4-OH	Ru
	35	C ₆ H ₄ -4-Pr ⁱ	C ₆ H ₄ -4-OH	Ru
	36	C ₆ H ₄ -4-Bu ^t	C ₆ H ₄ -4-OH	Ru
	37	C ₆ H ₄ -4-F	C ₆ H ₄ -4-OH	Ru
	38	C ₆ H ₄ -4-CF ₃	C ₆ H ₄ -4-OH	Ru
	39	CH ₂ -C ₆ H ₄ -4-Bu ^t	C ₆ H ₄ -4-OH	Os
	40	C ₆ H ₄ -4-Bu ^t	C ₆ H ₄ -4-OH	Os

Family 6

Family 6 is comprised of 8 compounds designed to assess the role of the methylene spacers in the bridge thiols, units correlated with the mobility and flexibility of the pendant arms in **1** and **H3** (Table 3, Figures 2 and S16). The hydrophobicity of the substituents was increased in the series H < Me < Prⁱ < Bu^t for compounds **33-36**, while derivatives **37** and **38** present polar F and CF₃ substituents. Two di-osmium compounds **39** and **40** were also synthesised allowing comparison with ruthenium analogues **1** and **36**.

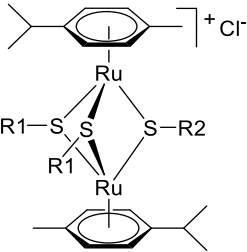
The results of the first screening for this family of compounds are presented in Figures 5 and 6 and Table 5. Compared to compound **1**, the presence of non-polar hydrophobic substituents (Me, Prⁱ, Bu^t) on two of the bridge thiols in **34-36** increased the anti-*Toxoplasma* activity, whereas polar substituents as F and CF₃ in **37** and **38** had an opposite effect. Nevertheless, irrespective of the nature of the substituents in *para* position, the di-ruthenium complexes **33-38** displayed lower HFF cytotoxicity than derivative **1**. Limited flexibility of the pendant arms and a reduced polarity of the substituents present on two of the bridge thiols seem to be associated with improved efficacy against *T. gondii*-β-gal and a relative innocuousness towards HFF host cells.

The change of the metal to osmium in compounds **39** and **40** provided contrasting results. Di-osmium compound **40** was clearly superior to its corresponding di-ruthenium analogue **1** both in terms of efficacy against *T. gondii*-β-gal and reduced HFF toxicity. However, no important differences were observed between **36** (di-ruthenium) and **39** (di-osmium), neither with respect to antiparasitic activity nor in relation to host cell viability impairment. These preliminary results suggest that the biological activity could be altered not only by modifying the substituents present on the bridge thiols but also by nature of the metal present in the main framework. Nevertheless, evaluating a larger number of osmium derivatives, or of structure related di-nuclear compounds based on other metals e.g., rhodium or iridium would be necessary to confirm this hypothesis.

Family 7

A group of ten derivatives formed Family 7 (Table 4, Figures 2 and S17). A previous study [50] identified symmetric compounds **H1** and **H2** (Figure 1) which exhibited interesting anti-*Toxoplasma* activity and low toxicity in HFF. These structures were the starting point for the evaluation of additional structurally related symmetric compounds. The hydrophobic Me and Bu^t groups of **H1** and **H2** were either removed in **41**, or replaced with polar fluoro and trifluoromethyl substituents, in compounds **42** and **43**, respectively. The role of the position (*meta* in **44**, *ortho* in **45**) and number (**46**) of the trifluoromethyl substituents was also assessed. Compounds **47-50** differ from the complementary analogues **43**, **41**, **H1** and **H2**, by the presence of methylene spacers on the bridge thiols. Compounds **42**, **44** and **46** were available in the laboratory from previous studies and only their purity was verified prior to assessing their biological activity (*Supporting information*).

Table 4. Structure of the compounds composing families 7 and 8.

	Compound	R1	R2
	Family 7 (R1 = R2)		
	H1 ^a		C ₆ H ₄ -4-Me
	H2 ^a		C ₆ H ₄ -4-Bu ^t
	41		C ₆ H ₅
	42		C ₆ H ₄ -4-F
	43		C ₆ H ₄ -4-CF ₃
	44		C ₆ H ₄ -3-CF ₃
	45		C ₆ H ₄ -2-CF ₃
	46		C ₆ H ₃ -3,5-(CF ₃) ₂
	47		CH ₂ -C ₆ H ₄ -4-CF ₃
	48		CH ₂ -C ₆ H ₅
	49		CH ₂ -C ₆ H ₄ -4-Me
	50		CH ₂ -C ₆ H ₄ -4-Bu ^t
	Family 8		
	51 ^b	CH ₂ -C ₆ H ₄ -4-CF ₃	C ₆ H ₄ -4-OH
	52 ^b	CH ₂ -C ₆ H ₄ -4-CF ₃	C ₆ H ₄ -4-NH ₂
	53 ^b	CH ₂ -C ₆ H ₄ -4-CF ₃	C ₆ H ₄ -4-CH ₂ -CO ₂ H
	54	CH ₂ -C ₆ H ₄ -4-CF ₃	C ₆ H ₄ -4-CH ₂ -CO ₂ CH ₃
	55	CH ₂ -C ₆ H ₄ -2-CF ₃	C ₆ H ₄ -4-OH
	56	CH ₂ -C ₆ H ₄ -2-CF ₃	C ₆ H ₄ -4-NH ₂

^apreviously reported in ref. [50], ^bpreviously reported in ref. [51].

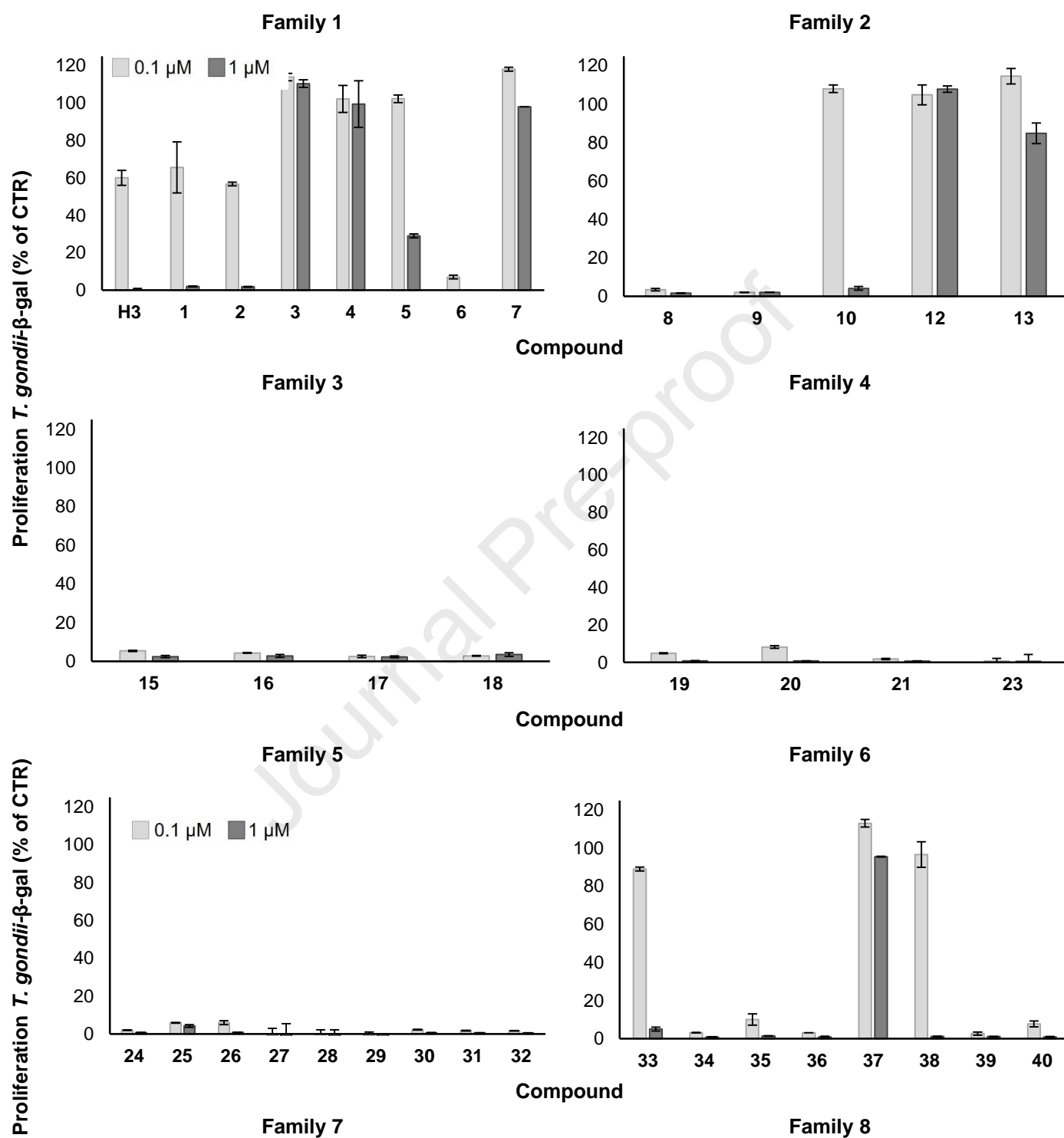
The primary screening results (Figures 5 and 6 and Table 5) showed that triphenyl compound **41** and analogues bearing trifluoromethyl groups **43-47** were highly efficient against *T. gondii*-β-gal, and inhibited parasite proliferation almost entirely already at 0.1 μM. However, trifluoromethyl substituted analogues **43-47** had a higher impact on HFF viability compared to **41**. The position and the number of the trifluoromethyl groups in **43-47** influenced HFF toxicity only marginally. *Para*-fluoro substituted compound **42** suppressed *T. gondii*-β-gal proliferation only when applied at 1 μM, while being more toxic for HFF compared to **41**. From the compounds with non-polar substituents and methylene

spacers on the pendant thiols, methyl derivative **49** was more efficient in preventing parasite proliferation compared to H- and Bu^t-substituted analogues **48** and **50**, being active already when applied at 0.1 μ M, but also with increased toxicity for HFF.

Summarizing, a more rigid structure in compounds **41-46** (without methylene groups on the pendant arms) favoured antiparasitic activity, but an increased number of polar trifluoromethyl groups led also to an increase in HFF toxicity. A fine balance of the polarity, size and number of the substituents is necessary to achieve a good compromise between antiparasitic activity and host cell cytotoxicity.

Family 8

Family 8 (Table 4, Figures 2 and S18) contains six members and was conceived based on lead derivative **H3** and considering the importance of the trifluoromethyl substituents in the compounds presented in family 7 (Table 4, Figures 2 and S16). The hydrophobic bulky Bu^t groups of two of the bridge thiols in **H3** were replaced with polar CF₃ groups, while the third thiol presents polar substituents as hydroxy (**51**), amino (**52**), carboxy (**53**) and ester (**54**). Mixed complexes **55** and **56** present two *ortho*-CF₃ substituted thiols, while the third thiol is substituted with a *para*-hydroxy (**55**) and -amino group (**56**). As shown in Figures 4 and 5, the replacement of one trifluoromethyl substituent in **47** with a hydroxy or amino group in **51** and **52**, respectively, significantly decreased antiparasitic activity (compounds active only when applied at 1 μ M), but had little impact on HFF cytotoxicity. The absence (**38**) or presence (**51**) of methylene spacers in the CF₃ substituted thiols did not substantially alter the anti-*Toxoplasma* activity and HFF cytotoxicity at 1 μ M. Similar to symmetric compound **45**, hydroxy and amino substituted derivatives **55** and **56**, were highly potent inhibitors of *T. gondii* proliferation even at 0.1 μ M, but were less toxic to HFF when applied at 1 μ M. Hydroxy and amino derivatives **51** and **52** with CF₃ groups, compared to their respective *para*-Bu^t-substituted analogues **1** and **2**, exhibited similar antiparasitic activity but slightly lower host cell toxicity. As previously observed for carboxy substituted compounds **3** and **4**, **53** did not display neither antiparasitic activity nor HFF toxicity. However, **54** with the carboxy group protected as methyl ester, presented increased toxicity against both *T. gondii*- β -gal and host cells; a similar effect was observed with ethyl ester derivative **18** as compared to the carboxy compound **3**.



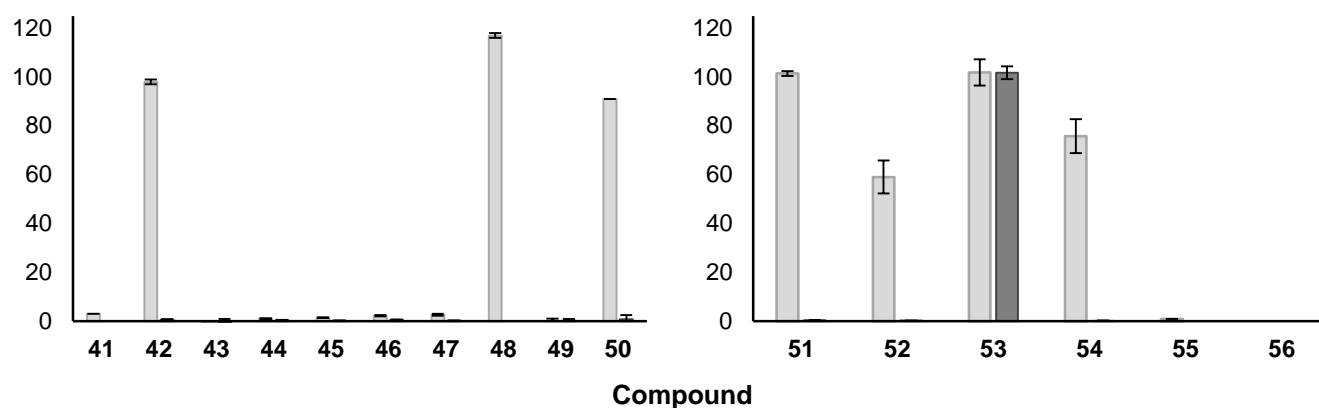
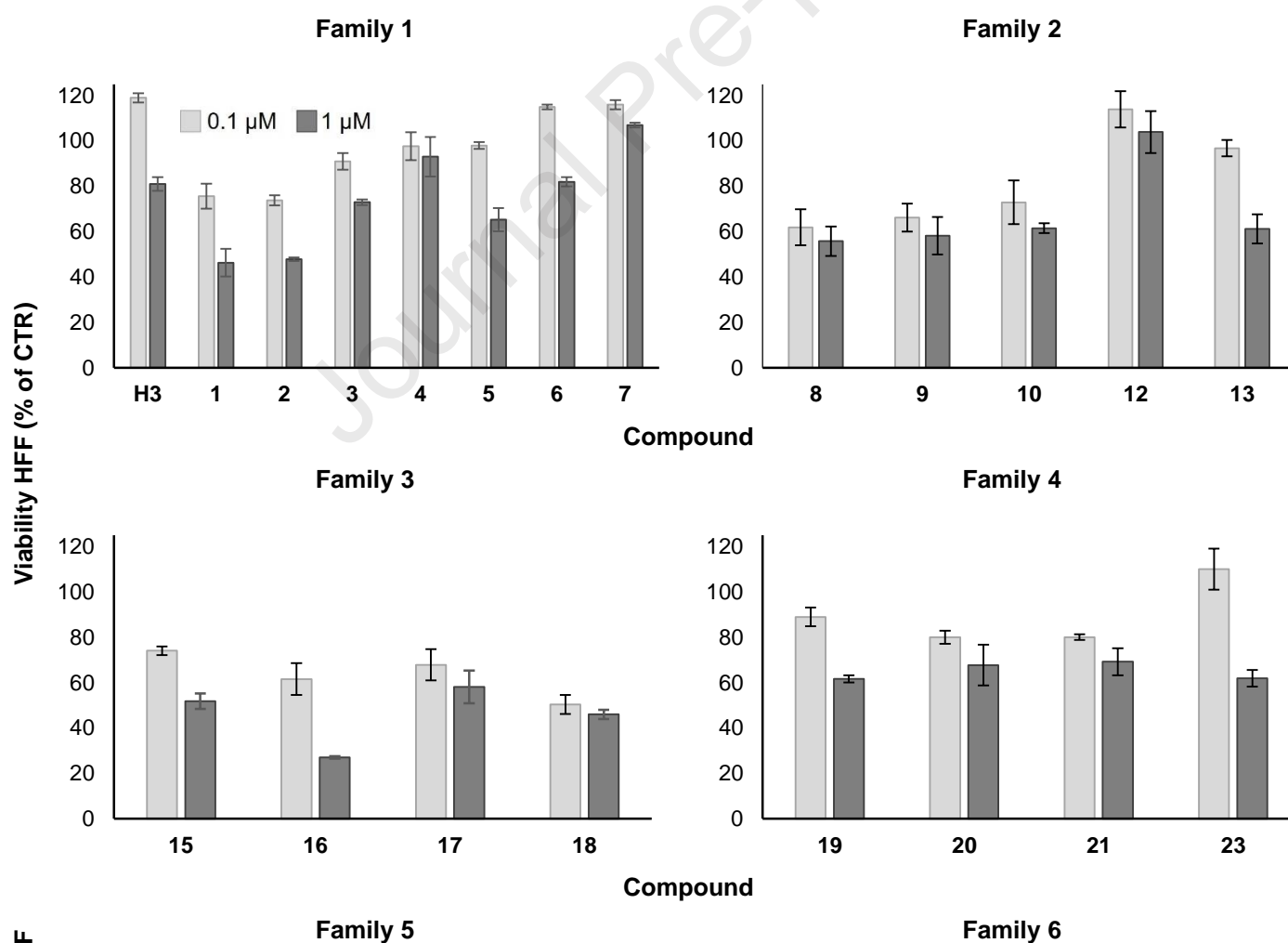


Figure 5. Primary screening: results for the 56 compounds assessed for anti-*T. gondii* activity. Compounds were organized into 8 families. *T. gondii* infected HFF cultures were treated at two concentrations 0.1 μM (light grey bars) and 1 μM (dark grey bars). Results are presented as mean of three replicates \pm standard deviation. Results are presented as percentage of *T. gondii*-β-gal proliferation relative to control (CTR) parasites treated with 0.01% or 0.1% DMSO (solvent only).



F

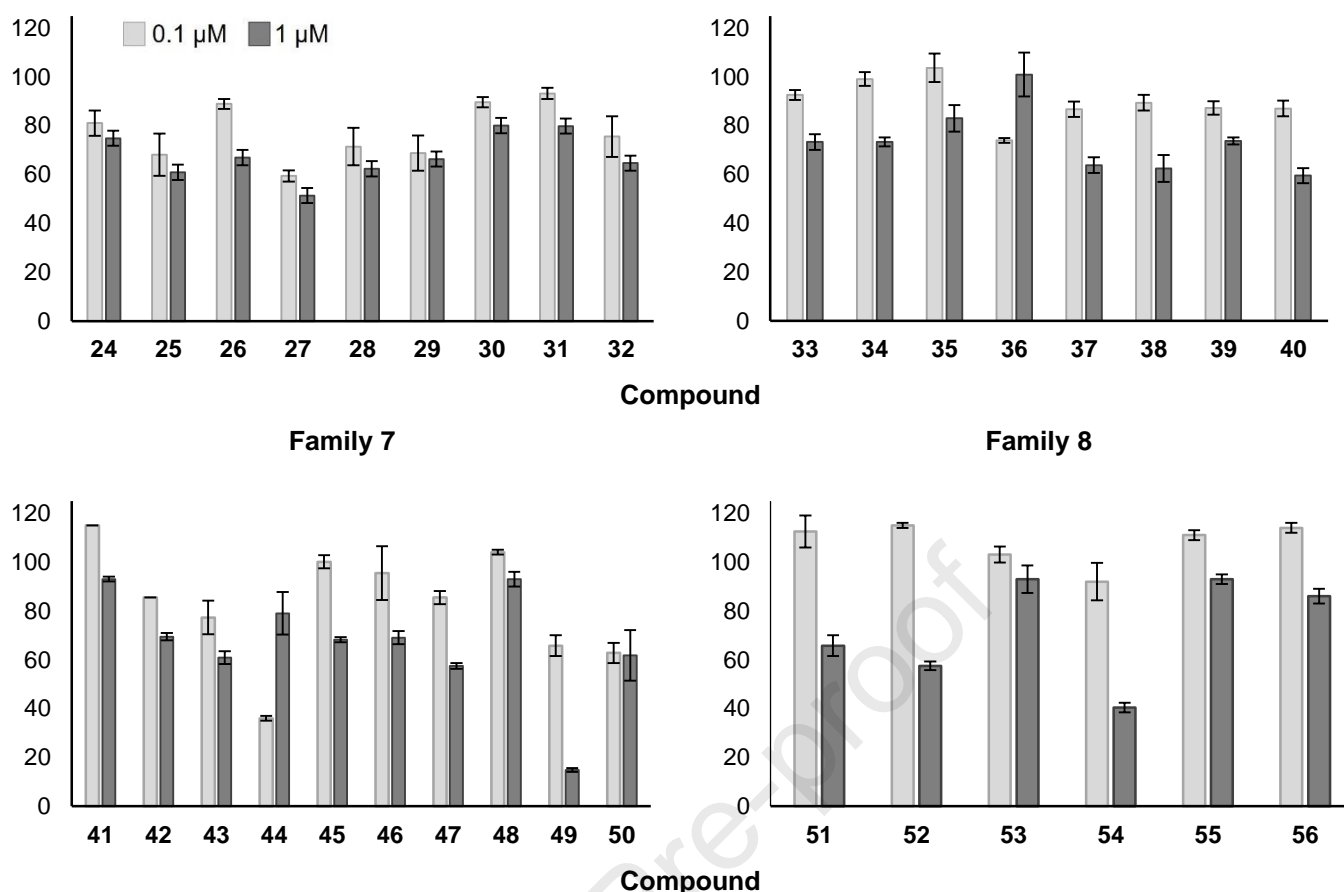


Figure 6. Primary screening: the 56 compounds were assessed with respect to activity against non-infected HFF. Compounds were organised into 8 families, and tested concentrations were 0.1 μM (light grey bars) and 1 μM (dark grey bars). Results are presented as mean of three replicates \pm standard deviation. Results are presented as percentage of HFF viability relative to a control (CTR), namely HFF treated with 0.01% or 0.1% DMSO (solvent only).

Table 5. Results of the primary efficacy/cytotoxicity screening.

Compound	HFF viability (%)		<i>T. gondii</i> β -gal growth (%)	
	0.1 μM	1 μM	0.1 μM	1 μM
H3^a	119 \pm 2	81 \pm 3	60 \pm 4	0 \pm 1
Family 1				
1^{b,d}	76 \pm 6	46 \pm 6	66 \pm 14	2 \pm 0
2^{b,d}	74 \pm 2	48 \pm 1	57 \pm 1	2 \pm 0
3^{b,d}	91 \pm 4	73 \pm 1	114 \pm 2	110 \pm 2
4	98 \pm 6	93 \pm 9	102 \pm 7	99 \pm 12
5^d	98 \pm 2	65 \pm 5	102 \pm 2	29 \pm 1
6^d	115 \pm 1	82 \pm 2	7 \pm 1	0 \pm 0
7	116 \pm 2	107 \pm 1	118 \pm 1	98 \pm 0
Family 2				
8^{c,d}	62 \pm 8	56 \pm 7	3 \pm 1	2 \pm 0
9^d	66 \pm 6	58 \pm 8	2 \pm 0	2 \pm 0
10^d	73 \pm 10	62 \pm 2	108 \pm 2	4 \pm 1
11^a	-	-	-	-

12	114 ± 8	104 ± 9	105 ± 5	108 ± 2
13	97 ± 4	61 ± 6	115 ± 4	85 ± 5
14^a	-	-	-	-
Family 3				
15^d	74 ± 2	52 ± 3	5 ± 0	2 ± 1
16	62 ± 7	27 ± 1	4 ± 0	3 ± 1
17^d	68 ± 7	58 ± 7	3 ± 1	2 ± 0
18	50 ± 4	46 ± 2	3 ± 0	4 ± 1
Family 4				
19^d	89 ± 4	62 ± 2	5 ± 0	1 ± 0
20^d	80 ± 3	68 ± 9	8 ± 1	1 ± 0
21^d	80 ± 1	69 ± 6	2 ± 0	1 ± 0
22^a	-	-	-	-
23^d	110 ± 9	62 ± 4	1 ± 1	1 ± 4
Family 5				
24^d	81 ± 5	75 ± 8	2 ± 0	1 ± 0
25^d	68 ± 9	61 ± 3	6 ± 0	4 ± 1
26^d	89 ± 2	67 ± 0	6 ± 1	1 ± 0
27^d	59 ± 2	51 ± 8	-1 ± 4	-3 ± 8
28^d	72 ± 8	62 ± 4	0 ± 3	-2 ± 4
29^d	69 ± 7	66 ± 7	-1 ± 2	-2 ± 2
30^d	90 ± 2	80 ± 3	2 ± 0	1 ± 0
31^d	93 ± 2	80 ± 6	2 ± 0	1 ± 0
32^d	76 ± 8	65 ± 3	2 ± 0	1 ± 0
Family 6				
33^d	93 ± 2	73 ± 3	89 ± 1	5 ± 1
34^d	99 ± 3	73 ± 2	3 ± 0	1 ± 0
35^d	104 ± 6	83 ± 5	10 ± 3	1 ± 0
36^d	74 ± 1	101 ± 9	3 ± 0	1 ± 0
37	87 ± 3	64 ± 3	113 ± 2	96 ± 0
38^d	89 ± 3	62 ± 6	97 ± 7	1 ± 0
39^d	87 ± 3	74 ± 1	3 ± 1	1 ± 0
40^d	87 ± 3	60 ± 3	8 ± 2	1 ± 0
Family 7				
H1^a	-	-	-	-
H2^a	-	-	-	-
41^d	115 ± 0	93 ± 1	3 ± 0	0 ± 0
42^d	85 ± 0	69 ± 2	98 ± 1	1 ± 0
43^d	77 ± 7	61 ± 3	-1 ± 0	0 ± 1
44^d	36 ± 1	79 ± 9	1 ± 0	0 ± 0
45^d	100 ± 3	68 ± 1	1 ± 0	0 ± 0
46^d	95 ± 11	69 ± 3	2 ± 0	1 ± 0
47^d	85 ± 3	57 ± 1	3 ± 0	0 ± 0
48^d	104 ± 1	93 ± 3	117 ± 1	0 ± 0
49	66 ± 4	15 ± 1	0 ± 1	0 ± 1
50^d	63 ± 4	62 ± 10	91 ± 0	1 ± 2

Family 8

51^{b,d}	112 ± 7	66 ± 4	101 ± 1	0 ± 0
52^{b,d}	115 ± 1	58 ± 2	59 ± 7	0 ± 0
53^b	103 ± 3	93 ± 6	102 ± 5	102 ± 3
54	92 ± 8	40 ± 2	76 ± 7	0 ± 0
55^d	111 ± 2	93 ± 2	1 ± 0	0 ± 0
56^d	114 ± 2	86 ± 3	0 ± 0	0 ± 0

^aCompound reported in ref. [50]. ^bCompound reported in ref. [51]. ^cCompound reported in ref. [79].

^dCompounds selected for the secondary screening.

The primary screening revealed that the compounds showing anti-*T. gondii* activity while remaining non-toxic against HFF are structurally varied. Free carboxy groups have a detrimental effect as compounds **3**, **4** and **7** (family 1) are admittedly non-toxic to the host cells but also show no antiproliferative activity on the parasite. Likewise, the presence of more than one hydroxy and amino substituents on the bridge thiols (family 2) is not a good option, as compounds bearing two polar groups (**8-10**) are active but also toxic to the host cells and those bearing three polar groups (**11-14**) are not active against the parasite. Interestingly, the protection of the polar groups OH, NH₂ or CO₂H as ester or amide (family 3) brings no benefit, as the HFF viability is significantly reduced when treated with compounds **15-18**. If the presence of one hydroxy group on one of the bridge thiols (family 4) appears to be important to the anti-parasitic activity, at this point of the study the influence if its position is not easy to define, even if compound presenting the OH group in *para* position (**1**) appear more toxic on the host cells and less active on the parasite compared to *meta* and *ortho* substituted analogues **19** and **20**.

Interestingly, the ether protection of the OH group (family 5, compounds **28-31**) appears to be a better option than the ester protection (**15**), while the nature of the protecting group (CH₃ or CF₃) as well as the position of the methoxy substituent impact the viability of the host cells. The presence of polar substituents F and especially CF₃ (**25** and **26**) on only one of the bridge thiols appears to be associated to increased toxicity on HFF. Removing the methylene spacer on two of the bridge thiols while maintaining the polar hydroxy group on the third thiol (family 6) is associated with an increased anti-*T. gondii* activity. One hydroxy group and two non-polar substituents such as Me, Prⁱ and Bu^t (**34**, **35** and **36**) are better options than three F or CF₃ both for the activity against the parasite and the toxicity on the host cells. Some of the observations made in the case of mixed compounds seem to apply also to the symmetric derivatives from family 7. Fluorine as substituent (compound **42**) led to a decreased activity against the parasite. The presence of methylene linkers on two of the bridge thiols appears to be associated to a decreased activity on *T. gondii* (**48**) or increased toxicity to HFF (compounds **47**, **49** and **50**). Compounds bearing polar CF₃ groups (**43**, **44**, **45** and **46**) seem a good compromise between anti-parasitic activity and effect on the host cell viability. The compounds from family 8 confirm some of the observations made previously: a free carboxy group on one of the bridge thiols (**53**) is to be

avoided, as well as the presence of methylene spacers on two of the bridging thiols (compounds **51** and **52**) or the protection of the carboxy group as an ester (**54**). Combining two CF₃ substituents on two of the bridge thiols with one polar hydroxy or amino group on the third thiol appears promising for ensuring both anti-*T. gondii* activity and reduced toxicity to the host cells.

2.2.3. Secondary screening

The selection criteria for a compound to enter secondary screening were: (i) over 95% inhibition of *T. gondii*-β-gal proliferation and (ii) not more than 49% viability impairment of HFF when applied at 1 μM. 39 compounds fulfilled these criteria and were chosen for the determination of IC₅₀ values against *T. gondii* and HFF viability assessments at 2.5 μM (Table 6). The IC₅₀ values against *T. gondii* ranged between 0.01 and 0.454 μM, and 30 compounds exhibited an IC₅₀ < 0.1 μM, which is significantly lower than the value measured for the standard drug pyrimethamine (0.326 μM) [51]. The viability of HFF at 2.5 μM compound concentration ranged between 1 and 89% when compared to non-treated cells. Eight compounds caused over 90% HFF cell death when applied at 2.5 μM, and 32 compounds caused viability loss higher than 30%.

Table 6. Secondary screening: determination of IC₅₀ (μM) values for *T. gondii*-β-gal and viability of HFF (as %-age in relation to solvent-treated controls) at 2.5 μM for the 39 compounds selected after the first screening. The 14 compounds selected for the tertiary screening (against murine B and T cells) are tagged with ^b and the corresponding measured values are shown in bold.

Compound	<i>T. gondii</i> -β-gal IC ₅₀ (μM)	[LI; LS] ^c	SE ^d	HFF viability at 2.5 μM (%) ^e	SD ^f
Pyrimethamine	0.326	[0.288; 0.396]	0.052	99	6
H3	0.079	[0.061; 0.102]	0.060	70	2
Family 1					
1^a	0.117	[0.098; 0.139]	0.051	56	6
2^a	0.153	[0.127; 0.185]	0.049	51	5
3^a	0.181	[0.274; 1.482]	0.954	99	2
5^a	0.316	[0.190; 0.526]	0.078	107	8
6^b	0.098	[0.066; 0.145]	0.085	72	3
Family 2					
8	0.115	[0.098; 0.134]	0.044	37	3
9	0.066	[0.046; 0.095]	0.126	19	1
10	0.294	[0.280; 0.308]	0.011	26	5
Family 3					
15	0.065	[0.041; 0.100]	0.092	16	5
17	0.014	[0.011; 0.032]	0.032	9	1
Family 4					
19	0.031	[0.024; 0.040]	0.07	16	2
20	0.050	[0.039; 0.062]	0.06	37	3

Journal Pre-proof					
21	0.038	[0.023; 0.060]	0.11	4	2
23	0.048	[0.031; 0.071]	0.11	31	4
Family 5					
24	0.052	[0.033; 0.083]	0.116	1	0
25	0.031	[0.021; 0.047]	0.119	34	7
26	0.013	[0.012; 0.014]	0.016	1	0
27	0.043	[0.037; 0.145]	0.184	36	7
28	0.056	[0.040; 0.079]	0.080	31	4
29^b	0.072	[0.035; 0.145]	0.214	59	5
30^b	0.078	[0.062; 0.097]	0.054	54	1
31	0.025	[0.017; 0.036]	0.088	40	10
32	0.039	[0.030; 0.052]	0.065	39	3
Family 6					
33	0.454	[0.370; 0.550]	0.046	31	12
34^b	0.072	[0.043; 0.119]	0.114	57	6
35^b	0.121	[0.067; 0.218]	0.133	56	4
36^b	0.041	[0.025; 0.065]	0.112	58	6
38^b	0.344	[0.302; 0.393]	0.031	70	6
39^b	0.062	[0.035; 0.112]	0.142	64	5
40	0.043	[0.034; 0.053]	0.05	49	3
Family 7					
41^b	0.072	[0.057; 0.092]	0.053	86	7
42^b	0.136	[0.093; 0.200]	0.099	55	3
43	0.031	[0.015; 0.078]	0.237	19	4
44	0.015	[0.010; 0.020]	0.057	26	16
45^b	0.017	[0.011; 0.026]	0.105	73	7
46	0.010	[0.008; 0.013]	0.045	6	5
47	0.016	[0.014; 0.017]	0.019	2	4
48^b	0.256	[0.202; 0.324]	0.052	89	5
50	0.268	[0.209; 0.345]	0.073	1	1
Family 8					
51	0.163	[0.008; 0.319]	1.7	9	2
52	0.063	[0.049; 0.082]	0.043	37	3
55^b	0.071	[0.054; 0.095]	0.063	84	3
56^b	0.056	[0.037; 0.087]	0.099	77	3

^aCompounds from family 1 which do not correspond to the first screening selection criteria, but for which the IC₅₀ values and viability of HFF were determined for comparison purpose.

^bCompounds selected for the third screening on immune cells.

^cValues at 95% confidence interval (CI); LI is the inferior limit of CI and LS is the superior limit of CI.

^dStandard error of the regression (SE), represents the average distance at which the measured values fall from the regression line.

^eControl HFF monolayers treated with 0.25 % DMSO exhibited 100% viability.

^fStandard deviation of the mean (six replicate experiments).

Compounds from family 1 showed a moderate to low host cell toxicity and IC₅₀ values against *T. gondii*-β-gal ranging from 0.117 to 0.316 μM. Interestingly, replacing the Cl⁻ (**2**) with a BF₄⁻ as

counterion (**6**) decreased HFF toxicity, but also improved antiparasitic activity. Interestingly, amino functionalized compound **6** appears to present rather similar activity and toxicity profile with the corresponding hydroxy derivative presenting the same BF_4^- counterion **H3**.

All compounds assigned to families 2, 3 and 4 strongly impaired the viability of HFF at 2.5 μM . For compounds belonging to family 2, the presence of two polar groups that can also take part in H-bonding interactions (derivatives **8** and **10** with two OH groups, and **9** with two NH_2 substituents) led to increased HFF toxicity compared to the mono-hydroxy and -amino compounds **1** and **2**. Interestingly, for diamino derivative **9** the *T. gondii* IC_{50} value was significantly lower compared to the IC_{50} values of the dihydroxy analogues **8** and **10** (0.066 μM vs 0.115 and 0.294 μM), but compound **9** was also more toxic for the host cells. The presence of the methylene spacer on one of the pendant arms also influenced the antiparasitic activity (**8** vs **10**). In family 3, both ester **15** and amide **17** were highly cytotoxic for HFF at 2.5 μM , and the effect was much stronger compared to the toxicity observed for the corresponding hydroxy and amino analogues **1** and **2**. In family 4, shifting the position of the OH group from *para* (**1**) to *meta* (**19**) or *ortho* (**20**) led to increased HFF toxicity. A similar effect was observed when replacing the *para* Bu^t groups (**1**) with less hydrophobic and bulky Me substituents (**23**). Interestingly, when applied at 2.5 μM *ortho*-methylenedihydroxy derivative **21** was significantly more toxic for the host cells compared to the *ortho*-hydroxy derivative **20**. All compounds from family 4 present methylene spacers on two of the pendant thiol arms.

Compounds **29** and **30** from family 5, moderately impaired HFF viability when applied at 2.5 μM (by 41 and 46%, respectively) and presented similar and low IC_{50} values against *T. gondii*- β -gal of 0.072 and 0.078 μM . In contrast, compounds **24** and **26** almost completely abolished HFF viability. Derivatives **25**, **27**, **28**, **31** and **32** applied at 2.5 μM reduced HFF viability in a 31 to 40% range, but *T. gondii* IC_{50} values were also lower, ranging from 0.013 to 0.056 μM .

The position of the methoxy group appeared to be important for the cytotoxicity against HFF, with *para* and *ortho* derivatives **28** and **31** being more toxic compared to the *meta*-substituted analogue **30**. For the *para*-substituted compounds **28** and **29**, the replacement of the hydrophobic methyl by the polar and bulkier trifluoromethyl reduced host cell toxicity.

Five of the seven compounds assigned to family 6 only moderately altered the viability of the host cells when tested at 2.5 μM , while **33** and **40** exhibited increased HFF toxicity. In this series of hydroxy analogues, a reduced flexibility of the substituents present on two of the thiols (no methylene spacers) had a positive effect on host cell viability. **36** presents the lowest and **38** the highest IC_{50} value against *T. gondii*- β -gal (0.041 and 0.344 μM , respectively), suggesting that more hydrophobic substituents (Bu^t vs CF_3) can favour antiparasitic activity. Interestingly, compounds **34**, **35** and **36** bearing hydrophobic substituents Me, Pr^i and Bu^t on two of the bridging thiols showed similar effects on the viability of the host cells (42-44% reduction), but IC_{50} values against *T. gondii* were not linearly dependent on the hydrophobicity/size of the substituents (IC_{50} values of 0.072, 0.121 and 0.041 μM ,

respectively). For the same peripheric ligands, ruthenium **36** and osmium **39** compounds showed comparable effects against *T. gondii*- β -gal and HFF. Replacement of the methyl groups on two of the thiols (**34**) by more polar and bulkier trifluoromethyl groups (**38**) strongly reduced the antiparasitic activity (IC_{50} values 0.072 vs 0.344 μ M, respectively).

From the compounds assigned to family 7, **43**, **44**, **46**, **47** and **50** strongly impaired HFF viability at 2.5 μ M (74-99%). The presence of three or six trifluoromethyl polar groups in *para* or *meta* positions, which can be involved in intermolecular interactions (H-bonding, polar) led to a considerable increase in HFF toxicity. Accordingly, HFF viability was almost completely abolished in the case of compounds **46**, **47** and **50**, suggesting that an increased number of polar groups (**46**) as well as the simultaneous presence of methylene spacers and of bulkier substituents in *para* position (**47** and **50**) increased HFF toxicity. Among the four compounds exhibiting low HFF toxicity, **48** showed the lowest, and **45** the highest activity against *T. gondii*- β -gal, with IC_{50} values of 0.256 and 0.017 μ M, respectively. Replacement of H with polar fluoro substituents (**41** vs **42**) reduced both the anti-*Toxoplasma* activity and the viability of HFF monolayers. Increased flexibility (presence of methylene spacers on the pendant substituents) and an increased number of polar substituents that can potentially interact with molecules from the environment, had a negative impact on HFF. Notably, the IC_{50} values of compounds **H1** and **H2** (0.034 and 0.062 μ M) are very low against *T. gondii*- β -gal, while the two compounds are non-toxic against the host cells (IC_{50} values on HFF of 800 and >1000 μ M, respectively) [50,57].

In family 8, the hydroxy and amino derivatives **51** and **52** differ from their analogues **55** and **56** by the position of the trifluoromethyl groups (*para* vs *ortho*) and the presence of methylene spacers on two of the bridging thiols. However, these structural differences had a strong influence on HFF toxicity. Both, **51** and **52** strongly affected HFF viability at 2.5 μ M. As previously observed, compounds exhibiting more rigid structures (the absence of the methylene linkers), as well as the presence of polar groups in positions that are less prone to intermolecular interactions (*ortho* vs *para*), were more likely to display reduced HFF toxicity. Thus, while **55** and **56** were both highly active against *T. gondii*- β -gal (IC_{50} values of 0.071 and 0.056 μ M, respectively), they presented reduced HFF toxicity at a concentration that was 35 times the *T. gondii* IC_{50} value.

Overall, the presence of one free (non-protected as ester or amide) OH or NH₂ group appeared to be important for antiparasitic activity, but the presence of two of these groups had detrimental effects on host cell viability. In addition, host cell toxicity was influenced by the position of the OH group. The position and number of other polar substituents such as CF₃ also affected the viability of the host cells. More rigid structures, lacking the methylene spacers on the pendant arms are to be favoured. During the secondary screening, 14 compounds, when applied at 2.5 μ M, reduced HFF viability by less than 50%. Compounds **6**, **29**, **30**, **34**, **35**, **36**, **38**, **39**, **41**, **42**, **45**, **48**, **55** and **56** were selected for the tertiary screening to study their impact on splenocyte viability and proliferation.

2.2.4. Tertiary screening

Previous studies [80,81] have proposed different types of ruthenium complexes as potential immunosuppressive agents to treat autoimmune diseases and allergic disorders. However, as this study aimed at developing ruthenium-based compounds for the treatment of *T. gondii* infection, any potential adverse reaction that particularly suppresses host immunity should be avoided. An ideal treatment strategy for toxoplasmosis would promote synergy between host immunity and the action of the applied antiparasitic drug [82].

The 14 selected compounds were evaluated for their immunosuppressive potential. B cells were stimulated with LPS [83,84] and T cells with Con A [85], and the effects of 0.1 and 0.5 μM of each compound were measured by assessing viability impairment by the AlamarBlue assay. For the compounds for which treatments at 0.5 μM did not induce more than 50% of T cell death and less than 90% of B cell death, the potential to inhibit the proliferative responses of B and T cells was further assessed by BrdU (5-bromo-2'-deoxyuridine) incorporation into DNA measured by ELISA (enzyme-linked immunosorbent assay) [51].

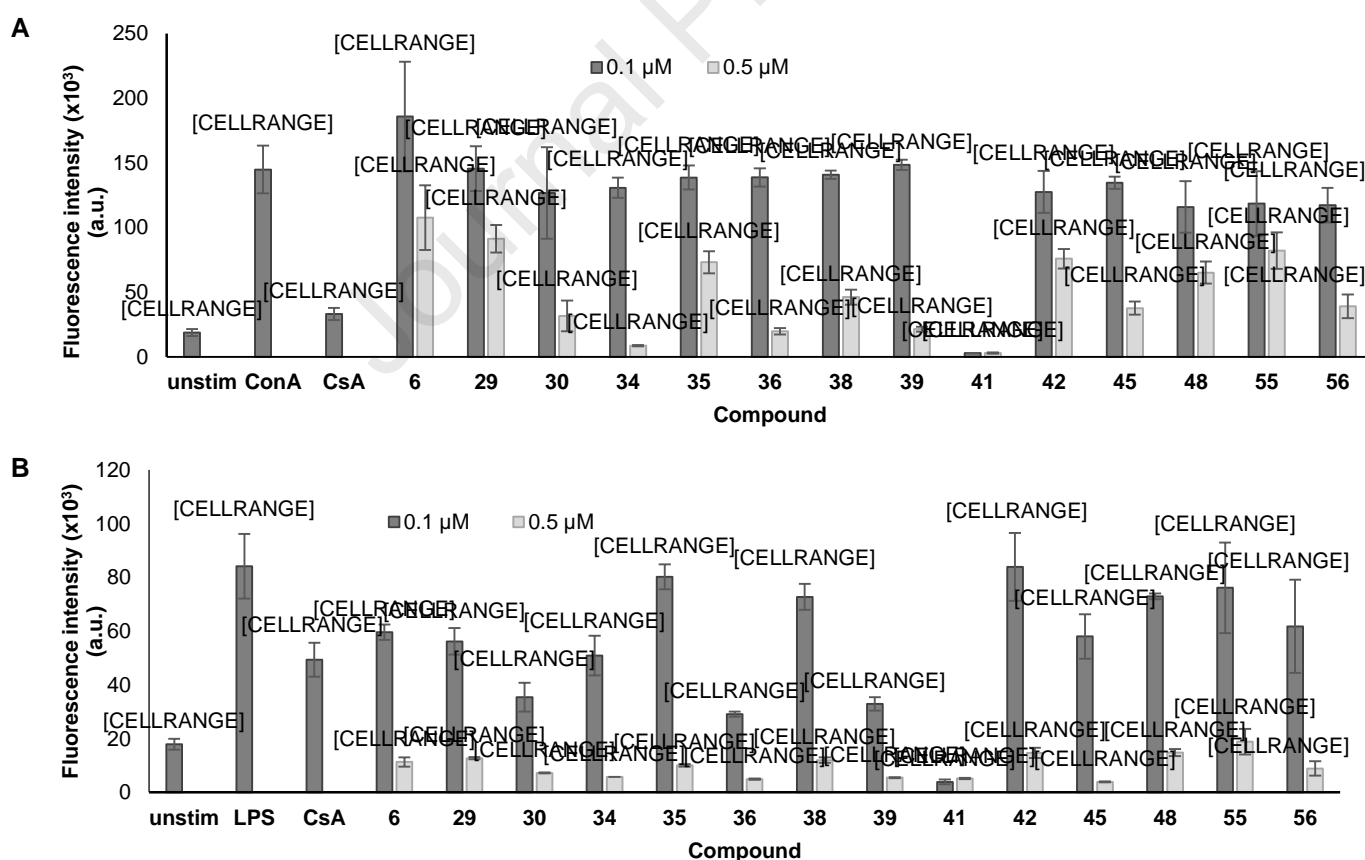


Figure 7. Tertiary screening of murine splenocyte cultures with 14 selected ruthenium complexes. The viability of splenocyte cultures stimulated with ConA (T cells, A) and LPS (B cells, B) was measured by AlamarBlue assay. Cultures were treated with 0.1 μM (dark grey bars) and 0.5 μM (light grey bars)

of each compound. Results are presented as fluorescence intensity at 590 nm (excitation at 530 nm), bars represent the mean emission of 4 replicates \pm standard deviation. The numbers above the bars indicate percentage in relation to the control (CTR = cells only stimulated with ConA (A) and cells only stimulated with LPS (B)). CsA (cyclosporin A, 1 μ M) was used as a known immunosuppressant.

As shown in Figure 7A and B, 13 out of the 14 tested compounds exerted dose-dependent effects on both B and T cells *in vitro*. The only exception was **41**, which was highly toxic and completely impaired T and B cell viability already at 0.1 μ M. The remaining 13 compounds did not exhibit excessive T cell toxicity at 0.1 μ M (viability ranging from 80 to 128% in relation to untreated cultures). B Cells appeared to be generally more susceptible, with relative values ranging from 35 to 100%. Toxicity was increased when treatments were carried out at 0.5 μ M, with relative viability values ranging from 6 to 74% for T cells and from 2 to 22% for B cells. Twelve compounds clearly exerted increased toxicity in B cells compared to T cells. In contrast, cyclosporin A (CsA), a known immunosuppressive drug used as control, had a more pronounced effect on T cells compared to B cells (23 vs 59% remaining relative viability).

Interestingly, for most compounds the toxicity values for HFF and T/B cells were not comparable. For instance, treatments of HFF with **55** and **56** at 2.5 μ M resulted in similarly moderate adverse effects (84 and 74% remaining viability, respectively, Table 6), while the application of 0.5 μ M of the same compounds resulted in severe viability impairment of B and T cells (residual relative viability of 22 and 11%, and 55 and 27%, respectively, Figure 7A and B, Tables S1 and S2). Likewise, **41** applied at 2.5 μ M did not display HFF toxicity (86% remaining viability, Table 6), but neither T nor B lymphocytes survived the treatments with **41** at 0.1 μ M (Figure 7A and B, Tables S1 and S2). These differences could be partly explained by the different metabolic states of HFF and splenocytes. HFF monolayers are largely confluent, exhibit contact-inhibition and are proliferating only slowly. ConA and LPS stimulated splenocyte cultures undergo rapid proliferation and are metabolically much more active. Nevertheless, these findings emphasize the necessity to include various cell-types for toxicity testing, especially considering that all nucleated cells are subject to infection with *T. gondii* [3].

Five compounds (**6**, **29**, **35**, **42** and **55**) were further investigated for their capacity to inhibit proliferative responses of T and B cells stimulated with ConA and LPS, respectively, using the BrdU (5-bromo-2'-deoxyuridine) incorporation into DNA measured by ELISA (enzyme-linked immunosorbent assay). The results (Figure 8A and B and Tables S3 and S4) demonstrate that T cell proliferation was not notably affected by any of the compounds at 0.1 μ M, and the same was true for compounds **29**, **42** and **55** at 0.5 μ M. However, treatments at 0.5 μ M with compounds **6** and **35** had a negative impact on T cell proliferative responses (Figure 8A). B cell proliferation was more strongly affected (Figure 8B). Compounds **6**, **29** and **35** exerted partial inhibition of B cell proliferation already at 0.1 μ M, and almost entirely abolished cell division at 0.5 μ M. The impairment effect was less

pronounced for compounds **42** and **55** at 0.5 μM , with residual relative proliferation occurring at 39 and 52% compared to non-treated controls, respectively. As observed in the viability tests, cyclosporin A had stronger effect on the proliferation of T cells compared to B cells (21 vs 60%).

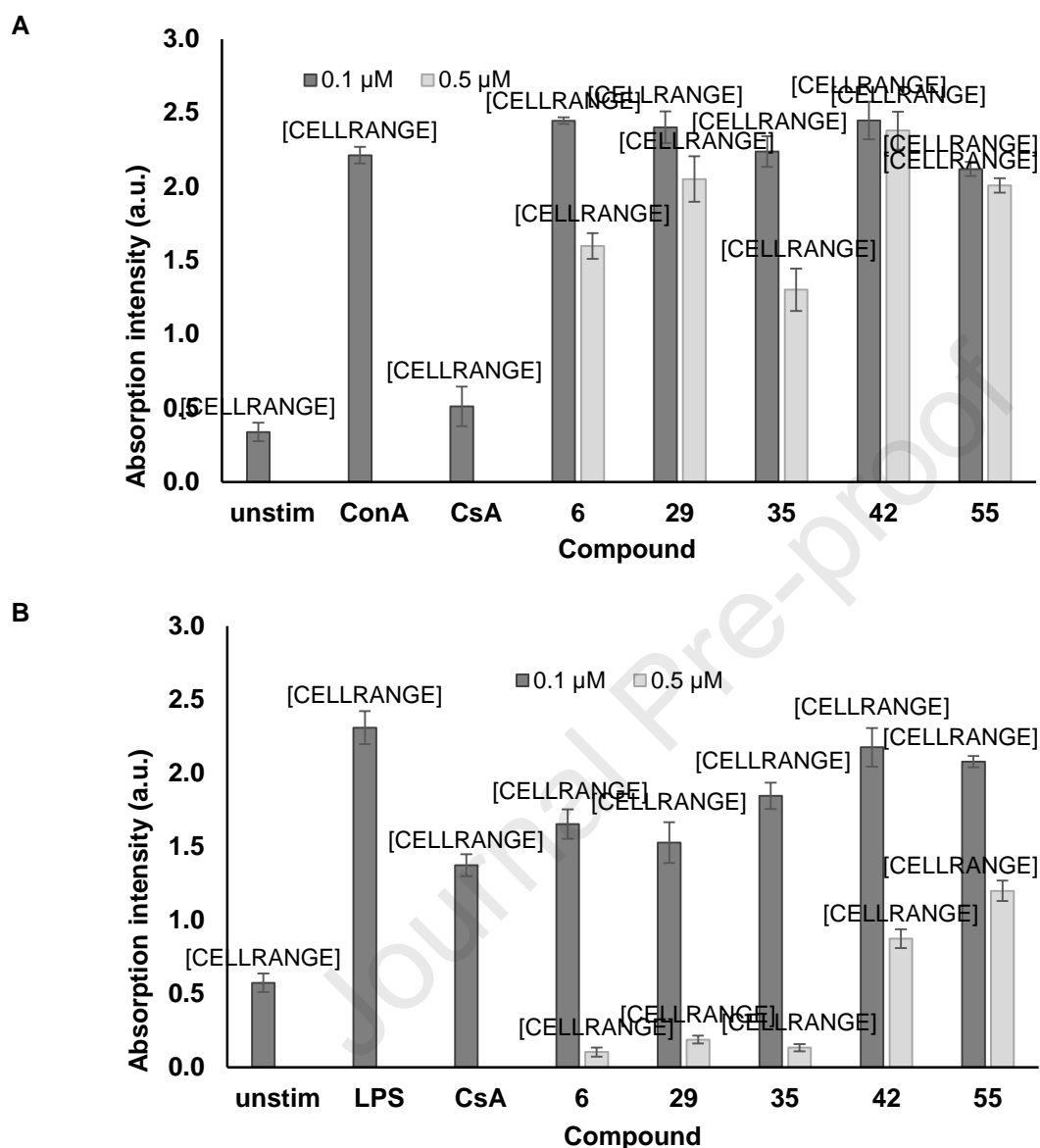


Figure 8. Tertiary screening: effects of compounds **6**, **29**, **35**, **42** and **55** on proliferative responses of murine splenocytes. T cell proliferation (A) was induced by the addition of ConA, B cell proliferation (B) was induced by adding LPS. Compounds were added at 0.1 μM (dark grey bars) and 0.5 μM (light grey bars), and BrdU incorporation into DNA was measured by ELISA assay. Bars represent standard deviation from the mean of three replicates. Results are presented as absorption intensity at 450 nm, the numbers above the bars indicate percentages in relation to the control (CTR = ConA or LPS plus solvent only). CsA (cyclosporin A, 1 μM) was used as a known immunosuppressant.

Compounds **6**, **29**, **35**, **42** and **55** affected the viability and the proliferation of B lymphocytes to a higher degree than T cells. However, when tested at a concentration close to its IC_{50} (0.1 μM), compound **55** neither affected the viability nor the proliferation of immune cells. In addition, HFF

remained largely viable when treated with 2.5 μM (35 times the *T. gondii* IC_{50} value). As a comparison, the standard drug pyrimethamine, which is currently used in the treatment of toxoplasmosis, was assessed similarly by BrdU ELISA at its *T. gondii* IC_{50} value (0.326 μM). Residual proliferation after treatments amounted up to 88% in ConA stimulated cultures (T cells) and 57% in LPS stimulated cultures (B cells). Based on these values, compound **55** performs slightly better than pyrimethamine and should be considered for further development.

The factors responsible for the observed differences in the susceptibility of B and T cells upon treatments with these compounds should be investigated. The increased susceptibility of B cells could be through interference in LPS binding to B cell receptors, inhibition of early activation events, or modulation of accessory cells such as macrophages which provide additional essential signals for B cell activation [86]. Despite presenting similar effects on the viability of T and B lymphocytes, compounds **35**, **42** and **55** exhibited divergent proliferation inhibition rates. This showed that the induced cellular events responsible for viability loss are different from those responsible for cell division inhibition, and/or that compounds **35** (family 6), **42** (family 7) and **55** (family 8) presenting various structural modifications do not share the same cellular targets. Overall, based on its selective antiparasitic activity and moderate direct effects on B and T cells, compound **55** appear as the most promising for further studies.

Even if this SAR study on trithiolato diruthenium derivatives did not provide conclusive rules for simultaneously improving specific anti-*Toxoplasma* activity and reducing general cytotoxicity, some structural elements that allowed selected compounds to possess high toxicity against *T. gondii* and general low toxicity against B- and T-cells were identified. These structural elements can constitute a starting point in the design of new, efficient and non toxic antiparasitic trithiolato dinuclear ruthenium compounds. Screening alternative counterions should be considered (e.g., BF_4^- in **6** vs Cl^- in **2**). The presence of a polar group (e.g., OH or NH_2 , but not CO_2H) appears to be favorable. Protection of the hydroxy group as ether could be interesting, but the nature of the protecting group might also be important e.g., a polar trifluoromethoxy (**29**) instead of methoxy group (**28**) should be favored. Reduced flexibility of groups pending on the bridge thiols by the absence of the methylene spacers (e.g., **35** and **55** vs **1/H3**) should be favored. The Bu^t substituents on two of the bridge thiols (**1/H3**) could be replaced by less hydrophobic/bulky Pr^i substituents (**35**) or by polar CF_3 groups (**55**), taking also into account the position of the substituents. Replacement of the hydrophobic Me and Bu^t in the symmetric **H1** and **H2** with polar fluoro groups in **42** also had positive effects.

Additional studies need to be carried out to elucidate which structural features of these compounds mediate antiparasitic efficacy, and what modifications could further reduce HFF toxicity, as well as alleviate viability impairment and antiproliferative effects on B and T cells. Antiparasitic efficacy is influenced by a direct targeting of metabolic functions of the parasite and whether these functions are essential, but also by the effects exerted on the host cell. In addition, these compounds undergo various

biophysical and biochemical processes, such as passage through several layers of membranes prior to reaching their target, and potential metabolic breakdown once they are located intracellularly, all of which will impact their stability and efficacy. Previous TEM studies in *Toxoplasma*, *Neospora* and in *Trypanosoma* demonstrated structural alterations in the parasite mitochondrion early after initiation of treatments with ruthenium complexes. In *Toxoplasma* and *Neospora*, these alterations included distinct changes in the mitochondrial matrix, and in the structural integrity of the parasite cristae, while HFF mitochondria remained largely unaltered [50,51,57]. In *T. brucei*, disruption of the mitochondrial membrane potential was demonstrated by tetramethylrhodamine ethyl ester assay, alterations in the trypanosome mitochondrion were evidenced by immunofluorescence employing an antibody against mitochondrial Hsp70 and Mitotracker labeling, and the mitochondrial matrix was converted into a translucent mass lacking any cristae as seen by TEM [58]. Future investigations should focus on elucidating the mechanism of action and on the identification of respective intracellular targets.

3. Conclusions

We report here a SAR study of a library of trithiolato-bridged dinuclear ruthenium(II)-arene compounds, which was tested for antiparasitic activity against *T. gondii*- β -gal tachyzoites, and cytotoxicity against HFF host cells and murine B and T cells. Systematic structural modifications of the parent compounds **H1**, **H2** and **H3** resulted in 56 compounds that were assigned to eight families, with successive structural variations, designed for increasing the antiparasitic activity and reduce the HFF and immune cell toxicity.

The activities of the compounds were assessed following a sequential three-step screening protocol. A primary screening for HFF toxicity and antiparasitic activity was undertaken with all 56 compounds at 0.1 and 1 μ M. 39 compounds, which, at a concentration of 1 μ M, inhibited parasite proliferation by more than 95% and impaired HFF viability by less than 49%, were chosen for the next step. This provided first insights into the biological effects of the different structural variations. For instance, the presence of free carboxy groups or more than one hydroxy and amino substituents on the bridge thiols is detrimental, while that of polar CF₃ groups appears beneficial. Methylene linkers in the pendant arms of two of the bridge thiols should be avoided. Combining one polar hydroxy or amino group on one bridge thiol and two CF₃ substituents on the other two thiols appears to be the best combination for ensuring both anti-*T. gondii* activity and reduced toxicity to the host cells.

The secondary screening included dose-response assays to determine the *T. gondii* IC₅₀ values, and the assessment of HFF toxicity of the compounds at 2.5 μ M. The 14 compounds that impaired HFF viability by less than 50% were subjected to the tertiary screening that focused on the effects on the viability and the proliferative potential in murine B and T cells. The results revealed that the presence

of one hydroxy group and polar CF₃ groups appears essential, as 9 out of these 14 compounds possess one or both of these two structural elements.

First the effects on the viability of immune cells were investigated at 0.1 and 0.5 μM, and subsequently the 5 compounds exhibiting the least detrimental effects against B and T cells were further evaluated for their potential to inhibit proliferative responses. The results showed that B cells exhibited a higher susceptibility than T cells. Compound **55** [$(\eta^6\text{-}p\text{-MeC}_6\text{H}_4\text{Pr}^i)_2\text{Ru}_2(\mu_2\text{-SC}_6\text{H}_4\text{-}o\text{-CF}_3)_2(\mu_2\text{-SC}_6\text{H}_4\text{-}p\text{-OH})\text{]Cl}$] emerged as a suitable candidate for further development.

Materials and Methods

Chemistry

The chemistry related general information, the experimental procedures used for the synthesis and the purification of the compounds, as well as characterization information (¹H and ¹³C NMR spectroscopy, mass spectrometry and elemental analysis data) are presented in detail in the *Supporting information*.

X-ray structure determination for **13**, **38**, **43** and **P13**

Experimental details regarding the X-ray structure determination for complexes **43** and **P13** are presented in the *Supporting information*.

Both the crystal of **13** and the crystal of **38** were mounted in air at ambient conditions. All measurements were made on a *RIGAKU Synergy S* area-detector diffractometer [87] using mirror optics monochromated Cu Kα radiation ($\lambda = 1.54184 \text{ \AA}$) [88].

For **13** the unit cell constants and an orientation matrix for data collection were obtained from a least-squares refinement of the setting angles of reflections in the range $5.724^\circ < 2\theta < 154.274^\circ$. For **13** a total of 4310 frames were collected using ω scans, with 0.05 seconds exposure time, a rotation angle of 0.5° per frame, a crystal-detector distance of 31.0 mm, at $T = 173(2) \text{ K}$. For **38** the unit cell constants and an orientation matrix for data collection were obtained from a least-squares refinement of the setting angles of reflections in the range $2.3^\circ < \theta < 77.1^\circ$. For **38** a total of 2900 frames were collected using ω scans, with 1.3 and 5.19 seconds exposure time, a rotation angle of 0.5° per frame, a crystal-detector distance of 34.0 mm, at $T = 173(2) \text{ K}$.

Data reduction was performed using the *CrysAlisPro* [87] program. The intensities were corrected for Lorentz and polarization effects, and an absorption correction based on the multi-scan method using SCALE3 ABSPACK in *CrysAlisPro* [87] was applied. Data collection and refinement parameters are given in Table S5. The structure was solved by direct methods using *SHELXT* [89], which revealed the positions of all non-hydrogen atoms of the title compound. All non-hydrogen atoms were refined anisotropically.

For **13** H-atoms were assigned in geometrically calculated positions and refined using a riding model where each H-atom was assigned a fixed isotropic displacement parameter with a value equal to 1.2Ueq of its parent atom (1.5Ueq for methyl groups). For **13** all H-atoms were placed in geometrically calculated positions and refined using a riding model where each H-atom was assigned a fixed isotropic displacement parameter with a value equal to 1.2Ueq of its parent atom (1.5Ueq for the methyl groups, the hydroxy group and water).

Refinement of the structures was carried out on F^2 using full-matrix least-squares procedures, which minimized the function $\Sigma w(F_o^2 - F_c^2)^2$. The weighting scheme was based on counting statistics and included a factor to down weight the intense reflections. All calculations were performed using the *SHELXL-2014/7* [90] program in OLEX2 [91]. For **38** about 6% of the unit cell volume is filled by heavily disordered co-crystallized solvent molecules. Its electron density was accounted for by the SQUEEZE procedure of PLATON [92].

Biological assessments

General

If not stated otherwise, the cell culture media were purchased from Gibco-BRL (Zurich, Switzerland) and the biochemical reagents were obtained from Sigma (St. Louis, MO, USA). The compounds used for *in vitro* studies were stored as 1 mM stock solutions in dimethylsulfoxide (DMSO) at -20°C . The HFF (human foreskin fibroblasts, SCRC-1041.1) were purchased from ATCC and were cultured and maintained as described earlier [93,94]. Tachyzoites of transgenic *T. gondii* strain containing a β -galactosidase reporter strain (*T. gondii*- β -gal, with Tg-RH background) were kindly provided by Prof. David Sibley (Washington University, St. Louis, USA) and were cultured in HFF, and were maintained and prepared for infections as described earlier [93,94].

Cytotoxicity in non-infected HFF

The cytotoxic effect was measured by AlamarBlue assay [49]. HFF were seeded into 96 well-plates at a density of 5×10^3 cells per well and monolayers were grown to confluency. For the screening, the medium was removed, and monolayers received 200 μL of fresh medium containing 0.1, 1, or 2.5 μM of each compound. Concentrations 0.1 and 1 μM were tested in triplicate wells, and 2.5 μM was assessed in sextuplicate. Non-treated HFF were also included and solvent controls contained DMSO at the corresponding concentrations of 0.01, 0.01 and 0.25%, respectively. Cultures were further maintained at $37^\circ\text{C}/5\% \text{ CO}_2$. After 72 h, the medium was removed, and cells were washed once with 200 μL phosphate buffered saline (PBS). Subsequently, 200 μL PBS containing resazurin (10 mg/mL dissolved in PBS) was added per well. Plates were read (excitation 530 nm, emission 590 nm wavelength) using an EnSpire multilabel reader (2300 EnSpire™ Multilabel Reader, Perkin-Elmer,

Turku, Finland) immediately (T0) or after 5 h (T5). The cytotoxicity values were calculated and represented as percentage of the respective DMSO control, which represented 100% of HFF viability.

Activity against *T. gondii*- β -gal tachyzoites

The transgenic *T. gondii*- β -gal strain cultured in HFF was used to assess tachyzoites proliferation inhibition [49]. HFF were seeded into 96 well-plates at a density of 5×10^5 cells per well and monolayers were grown to confluency. Monolayers were infected with 10^3 *T. gondii*- β -gal tachyzoites per well, and drugs (dilutions from the 1 mM stock solutions) were applied to cultures concomitantly with the infection.

Initial assessment of drug efficacy was realized by exposing parasite cultures to 0.1 and 1 μ M solutions of each compound in triplicate at 37°C/5% CO₂ over a period of 72 h, including DMSO solvent controls (at concentrations of 0.01 and 0.1%, respectively).

For IC₅₀ determinations, the compounds were added in the following concentrations: 0.007, 0.015, 0.03, 0.06, 0.12, 0.25, 0.5 and 1 μ M (sextuplicate for all), and cultures were maintained for 72 h at 37°C/5% CO₂. As solvent control, a solution of 0.1% DMSO (representing the highest DMSO concentration in the test) was used.

Subsequently the medium was removed, wells were washed once with 200 μ L PBS, and cells were permeabilized with 90 μ L PBS containing 0.05% Triton X-100 per well. After addition of 10 μ L of 5 mM chlorophenol red- β -D-galactopyranoside dissolved in PBS (CPRG, Roche Diagnostics, Rotkreuz, Switzerland), the absorption shift was measured at wavelength 570 nm at various timepoints on a EnSpire multilabel reader (2300 EnSpire™ Multilabel Reader, Perkin-Elmer, Turku, Finland). For the initial screening at 0.1 and 1 μ M, the activity, measured as the release of chlorophenol red over time, was calculated as percentage from the respective DMSO control, which represented 100% of *T. gondii*- β -gal growth. For the IC₅₀ assays, the activity measured as the release of chlorophenol red over time was proportional to the number of live parasites down to 50 per well as determined in pilot assays. IC₅₀ values were calculated after the logit-log transformation of the relative growth (RG, control = 1) according to the formula $\ln(RG/[1-RG]) = a \cdot \ln(\text{drug concentration}) + b$ and subsequent regression analysis by the corresponding software tool contained in the Excel software package (Microsoft, Seattle, WA, USA).

Activity against murine B and T cells stimulated with LPS and ConA, respectively

Spleen cell suspensions were prepared as previously described [51]. Female BALB/c mice were purchased from Charles River Laboratories (Sulzfeld, Germany) and were maintained in a common room under controlled temperature and a 14 h dark/10 h light cycle according to the standards set up by the animal welfare legislation of the Swiss Veterinary Office. The experimental protocol was approved by the Commission for Animal Experimentation of the Canton of Bern, Switzerland (Animal

license No. BE101/17). Mice were euthanized using isoflurane and CO₂, and spleens were aseptically removed from euthanized mice. Spleens from female BALB/c mice were removed and carefully minced by passing through 40 µm cell strainers. After lysis of red blood cells, splenocytes were counted and seeded in polystyrene 96 well flat bottom sterile plastic plates at 2×10^5 cells/100 µL/well. The impact of the selected compounds on splenic T and B cell viability was assessed by the AlamarBlue assay. Splenocyte cultures in 96 well-plates were used either unstimulated (negative control), or stimulated with ConA (5 µg/mL), LPS (10 µg/mL), ConA plus compound or LPS plus compound. The compounds were tested at 0.1 and 0.5 µM. Cyclosporine A (CsA) applied at 1 µM was included as control strong immunosuppressive compound. After 72 h of culture maintenance at 37°C/5% CO₂, resazurin (0.1 mg/mL) was added, and the fluorescence intensity was measured immediately (T0), and then after 5 hours (T5). Data are presented as mean of emission \pm standard deviation (SD) for the indicated numbers. Data comparisons between groups were examined using a Student's t-test (significant when $p < 0.001$). To measure the impact of compounds on the proliferative potential of B and T cells, the 5-bromo-2'-deoxyuridine (BrdU) cell proliferations assay was performed. Spleen cells were exposed to two concentrations (0.1 and 0.5 µM) of compounds in the presence of ConA (5 µg/mL) or LPS (10 µg/mL) for 72 h at 37°C/5% CO₂. Controls were splenocyte cultures with ConA or LPS devoided of drugs, or without treatment. Cyclosporine A (1 µM) treatment was also included in this assay. Proliferation was assessed with a BrdU cell proliferation kit (QIA58, Merck Millipore). BrdU label was added to the cultures 18 h prior the end of the incubation period, and incorporation of BrdU into DNA was measured by ELISA using peroxidase-conjugated anti-BrdU monoclonal antibody. Immediately after stopping the reaction, the absorbance was measured using dual wavelength of 450/540 nm, in an EnSpire multilabel reader (Perkin Elmer, Waltham). Data are presented as mean \pm SD for the indicated numbers. Data comparisons between groups were examined using a Student's t-test (significant when $p < 0.01$).

Associated Content

* *Supporting Information*

The *Supporting Information* is available free of charge on the website at DOI:

The chemistry experimental part with full description of experimental procedures and characterisation data, packing diagrams of the crystal structure and relevant bond parameters, stability data for the complexes in DMSO-d⁶ (.pdf).

Accession codes CCDC 2064260 (compound **13**), CCDC 2064259 (compound **38**), CCDC 2064257 (compound **43**) and CCDC 2064262 (compound **P13**) contain the supplementary crystallographic data for this paper. These data can be obtained free of charge via www.ccdc.cam.ac.uk/data_request/cif, or by emailing data_request@ccdc.cam.ac.uk, or by contacting The Cambridge Crystallographic Data Centre, 12 Union Road, Cambridge CB21EZ, UK; fax: +44 1223 336033.

Corresponding Authors

*E.P.: e-mail, paunescu_emilia@yahoo.com.

*A.H.: tel, +41-31-6312384; e-mail, andrew.hemphill@vetsuisse.unibe.ch. ORCID: 0000-0002-0622-2128

*J.F.: tel, +41-31-6314383; e-mail, julien.furrer@dcb.unibe.ch. ORCID: 0000-0003-2096-0618.

Notes

The authors declare no competing financial interest.

Acknowledgments

This work was financially supported by the Swiss Science National Foundation (SNF, Sinergia project CRSII5-173718 and project no. 310030_184662) and Y.A. was supported by a Swiss Governmental Excellence Fellowship. The X-ray crystal structure determination service unit of the Department of Chemistry, Biochemistry and Pharmaceutical Sciences of the University of Bern is acknowledged for measuring, solving, refining and summarizing the structures of compounds **13**, **38**, **43** and **P13**. The Synergy diffractometer was partially funded by the SNF within the R'Equip programme (project no. 206021_177033).

References

- [1] J. Muller, A. Hemphill, Drug target identification in protozoan parasites, *Expert Opin. Drug Discov.*, 11 (2016) 815-824. <https://doi.org/10.1080/17460441.2016.1195945>.
- [2] N.C. Smith, C. Goulart, J.A. Hayward, A. Kupz, C.M. Miller, G.G. van Dooren, Control of human toxoplasmosis, *Int. J. Parasitol.*, 51 (2021) 95-121. <https://doi.org/10.1016/j.ijpara.2020.11.001>.
- [3] J.P. Dubey, *Toxoplasmosis of animals and humans*, 2nd ed. ed., CRC Press, Boca Raton, 2010.
- [4] J.P. Dubey, A review of toxoplasmosis in wild birds, *Vet. Parasitol.*, 106 (2002) 121-153. [https://doi.org/10.1016/s0304-4017\(02\)00034-1](https://doi.org/10.1016/s0304-4017(02)00034-1).
- [5] A.M. Tenter, A.R. Heckeroth, L.M. Weiss, *Toxoplasma gondii*: from animals to humans, *Int. J. Parasitol.*, 30 (2000) 1217-1258. [https://doi.org/10.1016/S0020-7519\(00\)00124-7](https://doi.org/10.1016/S0020-7519(00)00124-7).
- [6] J. Flegr, J. Prandota, M. Sovickova, Z.H. Israili, Toxoplasmosis - a global threat. Correlation of latent Toxoplasmosis with specific disease burden in a set of 88 countries, *PLoS One*, 9 (2014) e90203. <https://doi.org/10.1371/journal.pone.0090203>.
- [7] P.R. Torgerson, P. Mastroiacovo, The global burden of congenital toxoplasmosis: a systematic review, *Bull. W. H. O.*, 91 (2013) 501-508. <https://doi.org/10.2471/BLT.12.111732>.
- [8] K. El Bissati, P. Levigne, J. Lykins, E.B. Adlaoui, A. Barkat, A. Berraho, M. Laboudi, B. El Mansouri, A. Ibrahimi, M. Rhajaoui, F. Quinn, M. Murugesan, F. Seghrouchni, J.E. Gomez-Marin, F. Peyron, R. McLeod, Global initiative for congenital toxoplasmosis: an observational and international comparative clinical analysis, *Emerging Microbes Infect.*, 7 (2018) 165. <https://doi.org/10.1038/s41426-018-0164-4>.
- [9] S. Fallahi, A. Rostami, M.N. Shiadeh, H. Behniafar, S. Paktinat, An updated literature review on maternal-fetal and reproductive disorders of *Toxoplasma gondii* infection, *J. Gynecol. Obstet. Hum. Reprod.*, 47 (2018) 133-140. <https://doi.org/10.1016/j.jogoh.2017.12.003>.

- [10] M.M. Hampton, Congenital Toxoplasmosis: a review, *Neonatal Netw.*, 34 (2015) 274-278. <https://doi.org/10.1891/0730-0832.34.5.274>.
- [11] J.G. Montoya, O. Liesenfeld, Toxoplasmosis, *Lancet*, 363 (2004) 1965-1976. [https://doi.org/10.1016/S0140-6736\(04\)16412-X](https://doi.org/10.1016/S0140-6736(04)16412-X).
- [12] C. Dard, P. Marty, M.P. Brenier-Pinchart, C. Garnaud, H. Fricker-Hidalgo, H. Pelloux, C. Pomares, Management of toxoplasmosis in transplant recipients: an update, *Expert Rev. Anti-Infect. Ther.*, 16 (2018) 447-460. <https://doi.org/10.1080/14787210.2018.1483721>.
- [13] M.A. Hussain, V. Stitt, E.A. Szabo, B. Nelán, Toxoplasma gondii in the food supply, *Pathogens*, 6 (2017). <https://doi.org/10.3390/pathogens6020021>.
- [14] I.R. Dunay, K. Gajurel, R. Dhakal, O. Liesenfeld, J.G. Montoya, Treatment of Toxoplasmosis: historical perspective, animal models, and current clinical practice, *Clin. Microbiol. Rev.*, 31 (2018) e00057-00017. <https://doi.org/10.1128/CMR.00057-17>.
- [15] A.J. Neville, S.J. Zach, X.F. Wang, J.J. Larson, A.K. Judge, L.A. Davis, J.L. Vennerstrom, P.H. Davis, Clinically available medicines demonstrating anti-Toxoplasma activity, *Antimicrob. Agents Chemother.*, 59 (2015) 7161-7169. <https://doi.org/10.1128/Aac.02009-15>.
- [16] P.H. Alday, J.S. Doggett, Drugs in development for toxoplasmosis: advances, challenges, and current status, *Drug Des. Dev. Ther.*, 11 (2017) 273-293. <https://doi.org/10.2147/Dddt.S60973>.
- [17] M. Montazeri, M. Sharif, S. Sarvi, S. Mehrzadi, E. Ahmadpour, A. Daryani, A systematic review of in vitro and in vivo activities of anti-Toxoplasma drugs and compounds (2006-2016), *Front. Microbiol.*, 8 (2017) 25. <https://doi.org/10.3389/fmicb.2017.00025>.
- [18] M.M. McFarland, S.J. Zach, X.F. Wang, L.P. Potluri, A.J. Neville, J.L. Vennerstrom, P.H. Davis, Review of experimental compounds demonstrating anti-Toxoplasma activity, *Antimicrob. Agents Chemother.*, 60 (2016) 7017-7034. <https://doi.org/10.1128/Aac.01176-16>.
- [19] M. Montazeri, S. Mehrzadi, M. Sharif, S. Sarvi, A. Tanzifi, S.A. Aghayan, A. Daryani, Drug resistance in Toxoplasma gondii, *Front. Microbiol.*, 9 (2018) 2587. <https://doi.org/10.3389/fmicb.2018.02587>.
- [20] Y.C. Ong, G. Gasser, Organometallic compounds in drug discovery: Past, present and future, *Drug Discovery Today: Technol.*, In Press, Corrected Proof (2019). <https://doi.org/10.1016/j.ddtec.2019.06.001>.
- [21] E.J. Anthony, E.M. Bolitho, H.E. Bridgewater, O.W.L. Carter, J.M. Donnelly, C. Imberti, E.C. Lant, F. Lermyte, R.J. Needham, M. Palau, P.J. Sadler, H. Shi, F.-X. Wang, W.-Y. Zhang, Z. Zhang, Metallodrugs are unique: opportunities and challenges of discovery and development *Chem. Sci.*, 11 (2020) 12888-12917 <https://doi.org/10.1039/D0SC04082G>.
- [22] C.G. Hartinger, N. Metzler-Nolte, P.J. Dyson, Challenges and opportunities in the development of organometallic anticancer drugs, *Organometallics*, 31 (2012) 5677-5685. <https://doi.org/10.1021/om300373t>.
- [23] R.W. Brown, C.J.T. Hyland, Medicinal organometallic chemistry - an emerging strategy for the treatment of neglected tropical diseases, *MedChemComm*, 6 (2015) 1230-1243. <https://doi.org/10.1039/C5MD00174A>.
- [24] Y.C. Ong, S. Roy, P.C. Andrews, G. Gasser, Metal compounds against neglected tropical diseases, *Chem. Rev.*, 119 (2019) 730-796. <https://doi.org/10.1021/acs.chemrev.8b00338>.
- [25] A. Frei, J. Zuegg, A.G. Elliott, M. Baker, S. Braese, C. Brown, F. Chen, C.G. Dowson, G. Dujardin, N. Jung, A.P. King, A.M. Mansour, M. Massi, J. Moat, H.A. Mohamed, A.K. Renfrew, P.J. Rutledge, P.J. Sadler, M.H. Todd, C.E. Willans, J.J. Wilson, M.A. Cooper, M.A.T. Blaskovich, Metal complexes as a promising source for new antibiotics, *Chem. Sci.*, 11 (2020) 2627-2639. <https://doi.org/10.1039/C9SC06460E>.
- [26] K.D. Mjos, C. Orvig, Metallodrugs in medicinal inorganic chemistry, *Chem. Rev.*, 114 (2014) 4540-4563. <https://doi.org/10.1021/cr400460s>.
- [27] B.S. Murray, P.J. Dyson, Recent progress in the development of organometallics for the treatment of cancer, *Curr. Opin. Chem. Biol.*, 56 (2020) 28-34. <https://doi.org/10.1016/j.cbpa.2019.11.001>.
- [28] M. Hanif, C.G. Hartinger, Anticancer metallodrugs: where is the next cisplatin?, *Future Med. Chem.*, 10 (2018) 615-617. <https://doi.org/10.4155/fmc-2017-0317>.
- [29] P. Zhang, P.J. Sadler, Advances in the design of organometallic anticancer complexes, *J. Organomet. Chem.*, 839 (2017) 5-14. <https://doi.org/10.1016/j.jorganchem.2017.03.038>.

- [30] R.G. Kenny, C.J. Marmion, Toward multi-targeted platinum and ruthenium drugs-a new paradigm in cancer drug treatment regimens?, *Chem. Rev.*, 119 (2019) 1058-1137. <https://doi.org/10.1021/acs.chemrev.8b00271>.
- [31] S. Parveen, F. Arjmand, S. Tabassum, Development and future prospects of selective organometallic compounds as anticancer drug candidates exhibiting novel modes of action, *Eur. J. Med. Chem.*, 175 (2019) 269-286. <https://doi.org/10.1016/j.ejmech.2019.04.062>.
- [32] J.X. Liang, H.J. Zhong, G. Yang, K. Vellaisamy, D.L. Ma, C.H. Leung, Recent development of transition metal complexes with in vivo antitumor activity, *J. Inorg. Biochem.*, 177 (2017) 276-286. <https://doi.org/10.1016/j.jinorgbio.2017.06.002>.
- [33] W. Su, Y. Li, P. Li, Design of Ru-arene complexes for antitumor drugs, *Mini Rev. Med. Chem.*, 18 (2018) 184-193. <https://doi.org/10.2174/1389557517666170510113453>.
- [34] S. Thota, D.A. Rodrigues, D.C. Crans, E.J. Barreiro, Ru(II) compounds: Next-generation anticancer metallotherapeutics?, *J. Med. Chem.*, 61 (2018) 5805-5821. <https://doi.org/10.1021/acs.jmedchem.7b01689>.
- [35] E.A. Hillard, G. Jaouen, Bioorganometallics: Future trends in drug discovery, analytical chemistry, and catalysis, *Organometallics*, 30 (2011) 20-27. <https://doi.org/10.1021/om100964h>.
- [36] J. Furrer, G. Süss-Fink, Thiolato-bridged dinuclear arene ruthenium complexes and their potential as anticancer drugs, *Coord. Chem. Rev.*, 309 (2016) 36-50. <https://doi.org/10.1016/j.ccr.2015.10.007>.
- [37] D. Gambino, L. Otero, Design of prospective antiparasitic metal-based compounds including selected organometallic cores, *Inorg. Chim. Acta*, 472 (2018) 58-75. <https://doi.org/10.1016/j.ica.2017.07.068>.
- [38] D. Dive, C. Biot, Ferrocene conjugates of chloroquine and other antimalarials: the development of ferroquine, a new antimalarial, *ChemMedChem*, 3 (2008) 383-391. <https://doi.org/10.1002/cmdc.200700127>.
- [39] M. Navarro, W. Castro, C. Biot, Bioorganometallic compounds with antimalarial targets: Inhibiting hemozoin formation, *Organometallics*, 31 (2012) 5715-5727. <https://doi.org/10.1021/om300296n>.
- [40] C. Biot, F. Nosten, L. Fraisse, D. Ter-Minassian, J. Khalife, D. Dive, The antimalarial ferroquine: from bench to clinic, *Parasite*, 18 (2011) 207-214. <https://doi.org/10.1051/parasite/2011183207>.
- [41] E.V. Capparelli, R. Bricker-Ford, M.J. Rogers, J.H. McKerrow, S.L. Reed, Phase I clinical trial results of auranofin, a novel antiparasitic agent, *Antimicrob. Agents Chemother.*, 61 (2017) e01947-01916. <https://doi.org/10.1128/AAC.01947-16>.
- [42] J.A. Portes, T.G. Souza, T.A. dos Santos, L.L. da Silva, T.P. Ribeiro, M.D. Pereira, A. Horn, Jr., C. Fernandes, R.A. DaMatta, W. de Souza, S.H. Seabra, Reduction of *Toxoplasma gondii* development due to inhibition of parasite antioxidant enzymes by a dinuclear iron(III) compound, *Antimicrob. Agents Chemother.*, 59 (2015) 7374-7386. <https://doi.org/10.1128/AAC.00057-15>.
- [43] V.M. de Assis, L.C. Visentin, F.S. de Souza, R.A. DaMatta, A. Horn, C. Fernandes, Synthesis, crystal structure and relevant antiproliferative activity against *Toxoplasma gondii* of a new binuclear Co(II) complex, *Inorg. Chem. Commun.*, 67 (2016) 47-50. <https://doi.org/10.1016/j.inoche.2016.02.017>.
- [44] J.A. Portes, C.S. Motta, N.F. Azeredo, C. Fernandes, A. Horn, Jr., W. De Souza, R.A. DaMatta, S.H. Seabra, In vitro treatment of *Toxoplasma gondii* with copper(II) complexes induces apoptosis-like and cellular division alterations, *Vet. Parasitol.*, 245 (2017) 141-152. <https://doi.org/10.1016/j.vetpar.2017.04.002>.
- [45] L.C. Batista, F.S. de Souza, V.M. de Assis, S.H. Seabra, A.J. Bortoluzzi, M.N. Renno, A. Horn, R.A. DaMatta, C. Fernandes, Antiproliferative activity and conversion of tachyzoite to bradyzoite of *Toxoplasma gondii* promoted by new zinc complexes containing sulfadiazine, *RSC Adv.*, 5 (2015) 100606-100617. <https://doi.org/10.1039/C5RA17690E>.
- [46] J.D. Portes, N.F.B. Azeredo, P.G.T. Siqueira, T.G. de Souza, C. Fernandes, A. Horn, D.R.S. Candela, W. de Souza, R.A. DaMatta, S.H. Seabra, A new iron(III) complex-containing sulfadiazine inhibits the proliferation and induces cystogenesis of *Toxoplasma gondii*, *Parasitol. Res.*, 117 (2018) 2795-2805. <https://doi.org/10.1007/s00436-018-5967-7>.
- [47] S. Carradori, D. Secci, B. Bizzarri, P. Chimenti, C. De Monte, P. Guglielmi, C. Campestre, D. Rivanera, C. Bordon, L. Jones-Brando, Synthesis and biological evaluation of anti-*Toxoplasma gondii*

- activity of a novel scaffold of thiazolidinone derivatives, *J. Enzyme Inhib. Med. Chem.*, 32 (2017) 746-758. <https://doi.org/10.1080/14756366.2017.1316494>.
- [48] A. Baramée, A. Coppin, M. Mortuaire, L. Pelinski, S. Tomavo, J. Brocard, Synthesis and in vitro activities of ferrocenic aminohydroxynaphthoquinones against *Toxoplasma gondii* and *Plasmodium falciparum*, *Bioorg. Med. Chem.*, 14 (2006) 1294-1302. <https://doi.org/10.1016/j.bmc.2005.09.054>.
- [49] F. Barna, K. Debache, C.A. Vock, T. Kuster, A. Hemphill, In vitro effects of novel ruthenium complexes in *Neospora caninum* and *Toxoplasma gondii* tachyzoites, *Antimicrob. Agents Chemother.*, 57 (2013) 5747-5754. <https://doi.org/10.1128/AAC.02446-12>.
- [50] A.P. Basto, J. Muller, R. Rubbiani, D. Stibal, F. Giannini, G. Suss-Fink, V. Balmer, A. Hemphill, G. Gasser, J. Furrer, Characterization of the activities of dinuclear thiolato-bridged arene ruthenium complexes against *Toxoplasma gondii*, *Antimicrob. Agents Chemother.*, 61 (2017). <https://doi.org/10.1128/AAC.01031-17>.
- [51] O. Desiatkina, E. Paunescu, M. Mosching, N. Anghel, G. Boubaker, Y. Amdouni, A. Hemphill, J. Furrer, Coumarin-tagged dinuclear trithiolato-bridged ruthenium(II)arene complexes: photophysical properties and antiparasitic activity, *Chembiochem*, 21 (2020) 2818-2835. <https://doi.org/10.1002/cbic.202000174>.
- [52] V. Studer, N. Anghel, O. Desiatkina, T. Felder, G. Boubaker, Y. Amdouni, J. Ramseier, M. Hungerbühler, C. Kempf, J.T. Heverhagen, A. Hemphill, N. Ruprecht, J. Furrer, E. Paunescu, Conjugates containing two and three trithiolato-bridged dinuclear ruthenium(II)-arene units as in Vitro antiparasitic and anticancer agents, *Pharmaceuticals*, 13 (2020) 471. <https://doi.org/10.3390/ph13120471>.
- [53] R.M. Andrade, J.D. Chaparro, E. Capparelli, S.L. Reed, Auranofin is highly efficacious against *Toxoplasma gondii* in vitro and in an in vivo experimental model of acute toxoplasmosis, *PLoS Negl. Trop. Dis.*, 8 (2014) e2973. <https://doi.org/10.1371/journal.pntd.0002973>.
- [54] C. Rocha-Roa, D. Molina, N. Cardona, A perspective on thiazolidinone scaffold development as a new therapeutic strategy for Toxoplasmosis, *Front. Cell Infect. Microbiol.*, 8 (2018) 360. <https://doi.org/10.3389/fcimb.2018.00360>.
- [55] S. Romand, M. Pudney, F. Derouin, In vitro and in vivo activities of the hydroxynaphthoquinone atovaquone alone or combined with pyrimethamine, sulfadiazine, clarithromycin, or minocycline against *Toxoplasma gondii*, *Antimicrob. Agents Chemother.*, 37 (1993) 2371-2378. <https://doi.org/10.1128/aac.37.11.2371>.
- [56] T. Kuster, N. Lense, F. Barna, A. Hemphill, M.K. Kindermann, J.W. Heinicke, C.A. Vock, A new promising application for highly cytotoxic metal compounds: eta(6)-arene ruthenium(II) phosphite complexes for the treatment of alveolar Echinococcosis, *J. Med. Chem.*, 55 (2012) 4178-4188. <https://doi.org/10.1021/jm300291a>.
- [57] A.P. Basto, N. Anghel, R. Rubbiani, J. Muller, D. Stibal, F. Giannini, G. Suss-Fink, V. Balmer, G. Gasser, J. Furrer, A. Hemphill, Targeting of the mitochondrion by dinuclear thiolato-bridged arene ruthenium complexes in cancer cells and in the apicomplexan parasite *Neospora caninum*, *Metallomics*, 11 (2019) 462-474. <https://doi.org/10.1039/c8mt00307f>.
- [58] J. Jelk, V. Balmer, D. Stibal, F. Giannini, G. Suss-Fink, P. Butikofer, J. Furrer, A. Hemphill, Anti-parasitic dinuclear thiolato-bridged arene ruthenium complexes alter the mitochondrial ultrastructure and membrane potential in *Trypanosoma brucei* bloodstream forms, *Exp. Parasitol.*, 205 (2019) 107753. <https://doi.org/10.1016/j.exppara.2019.107753>.
- [59] M. Mbaba, T.M. Golding, G.S. Smith, Recent advances in the biological investigation of organometallic platinum-group metal (Ir, Ru, Rh, Os, Pd, Pt) complexes as antimalarial agents, *Molecules*, 25 (2020). <https://doi.org/10.3390/molecules25225276>.
- [60] L.K. Batchelor, P.J. Dyson, Extrapolating the fragment-based approach to inorganic drug discovery, *Trends Chem.*, 1 (2019) 644-655. <https://doi.org/10.1016/j.trechm.2019.05.001>.
- [61] C.N. Morrison, K.E. Prosser, R.W. Stokes, A. Cordes, N. Metzler-Nolte, S.M. Cohen, Expanding medicinal chemistry into 3D space: metallofragments as 3D scaffolds for fragment-based drug discovery, *Chem. Sci.*, 11 (2020) 1216-1225. <https://doi.org/10.1039/C9SC05586J>.
- [62] Y. Zhao, Y. Kang, F. Xu, W. Zheng, Q. Luo, Y. Zhang, F. Jiaa, F. Wang, Advances in Inorganic Chemistry, Volume: Medicinal Chemistry, in: R.v.E. Peter J. Sadler (Ed.), 2020 pp. 257-285.

- [63] M.J. Chow, C. Licon, D. Yuan Qiang Wong, G. Pastorin, C. Gaiddon, W.H. Ang, Discovery and investigation of anticancer ruthenium-arene Schiff-base complexes via water-promoted combinatorial three-component assembly, *J. Med. Chem.*, 57 (2014) 6043-6059. <https://doi.org/10.1021/jm500455p>.
- [64] S.P. Mulcahy, K. Grundler, C. Frias, L. Wagner, A. Prokop, E. Meggers, Discovery of a strongly apoptotic ruthenium complex through combinatorial coordination chemistry, *Dalton Trans.*, 39 (2010) 8177-8182. <https://doi.org/10.1039/c0dt00034e>.
- [65] M.F. Mosquillo, P. Smircich, M. Ciganda, A. Lima, D. Gambino, B. Garat, L. Pérez-Díaz, Comparative high-throughput analysis of the *Trypanosoma cruzi* response to organometallic compounds, *Metallomics*, 12 (2020) 813-828. <https://doi.org/10.1039/D0MT00030B>.
- [66] M.F. Mosquillo, P. Smircich, A. Lima, S.A. Gehrke, G. Scalese, I. Machado, D. Gambino, B. Garat, L. Perez-Diaz, High throughput approaches to unravel the mechanism of action of a new vanadium-based compound against *Trypanosoma cruzi*, *Bioinorg. Chem. Appl.*, 2020 (2020) 1634270. <https://doi.org/10.1155/2020/1634270>.
- [67] S.M. Meier-Menches, C. Gerner, W. Berger, C.G. Hartinger, B.K. Keppler, Structure-activity relationships for ruthenium and osmium anticancer agents - towards clinical development, *Chem. Soc. Rev.*, 47 (2018) 909-928. <https://doi.org/10.1039/c7cs00332c>.
- [68] L.I. Rylands, A. Welsh, K. Maepa, T. Stringer, D. Taylor, K. Chibale, G.S. Smith, Structure-activity relationship studies of antiplasmodial cyclometallated ruthenium(II), rhodium(III) and iridium(III) complexes of 2-phenylbenzimidazoles, *Eur. J. Med. Chem.*, 161 (2019) 11-21. <https://doi.org/10.1016/j.ejmech.2018.10.019>.
- [69] E.L. Cedillo-Gutierrez, L.F. Hernandez-Ayala, C. Torres-Gutierrez, M. Reina, M. Flores-Alamo, J.C. Carrero, V.M. Ugalde-Saldivar, L. Ruiz-Azuara, Identification of descriptors for structure-activity relationship in ruthenium (II) mixed compounds with antiparasitic activity, *Eur. J Med. Chem.*, 189 (2020) 112084. <https://doi.org/10.1016/j.ejmech.2020.112084>.
- [70] A. Habtemariam, M. Melchart, R. Fernandez, S. Parsons, I.D. Oswald, A. Parkin, F.P. Fabbiani, J.E. Davidson, A. Dawson, R.E. Aird, D.I. Jodrell, P.J. Sadler, Structure-activity relationships for cytotoxic ruthenium(II) arene complexes containing N,N-, N,O-, and O,O-chelating ligands, *J. Med. Chem.*, 49 (2006) 6858-6868. <https://doi.org/10.1021/jm060596m>.
- [71] D. Havrylyuk, B.S. Howerton, L. Nease, S. Parkin, D.K. Heidary, E.C. Glazer, Structure-activity relationships of anticancer ruthenium(II) complexes with substituted hydroxyquinolines, *Eur. J. Med. Chem.*, 156 (2018) 790-799. <https://doi.org/10.1016/j.ejmech.2018.04.044>.
- [72] W. Ginzinger, G. Muhlgassner, V.B. Arion, M.A. Jakupiec, A. Roller, M. Galanski, M. Reithofer, W. Berger, B.K. Keppler, A SAR study of novel antiproliferative ruthenium and osmium complexes with quinoxalinone ligands in human cancer cell lines, *J. Med. Chem.*, 55 (2012) 3398-3413. <https://doi.org/10.1021/jm3000906>.
- [73] A.F. Ibaño, M. Gras, B. Therrien, G. Süss-Fink, O. Zava, P.J. Dyson, Thiolato-bridged arene-ruthenium complexes: synthesis, molecular structure, reactivity, and anticancer activity of the dinuclear complexes [(arene)₂Ru₂(SR)₂Cl₂], *Eur. J. Inorg. Chem.*, (2012) 1531-1535. <https://doi.org/10.1002/ejic.201101057>.
- [74] F. Giannini, L.E.H. Paul, J. Furrer, B. Therrien, G. Süss-Fink, Highly cytotoxic diruthenium trithiolato complexes of the type [(η⁶-p-MeC₆H₄Pr)₂Ru-2(μ²-SR)₃](+): synthesis, characterization, molecular structure and in vitro anticancer activity, *New J. Chem.*, 37 (2013) 3503-3511. <https://doi.org/10.1039/C3NJ00476G>.
- [75] F. Giannini, J. Furrer, A.F. Ibaño, G. Süss-Fink, B. Therrien, O. Zava, M. Baquie, P.J. Dyson, P. Stepnicka, Highly cytotoxic trithiophenolatodiruthenium complexes of the type [(η⁶-p-MeC₆H₄Pr)₂Ru₂(SC₆H₄-p-X)₃]⁺: synthesis, molecular structure, electrochemistry, cytotoxicity, and glutathione oxidation potential, *J. Biol. Inorg. Chem.*, 17 (2012) 951-960. <https://doi.org/10.1007/s00775-012-0911-2>.
- [76] F. Giannini, J. Furrer, G. Süss-Fink, C.M. Clavel, P.J. Dyson, Synthesis, characterization and in vitro anticancer activity of highly cytotoxic trithiolato diruthenium complexes of the type [(η⁶-p-(MeC₆H₄Pr)-Pr-i)₂Ru-2(μ²-SR₁)(2)(μ²-SR₂)](+) containing different thiolato bridges, *J. Organomet. Chem.*, 744 (2013) 41-48. <https://doi.org/10.1016/j.jorganchem.2013.04.049>.
- [77] D. Stibal, G. Süss-Fink, B. Therrien, Crystal structure of (μ⁴-hydroxy-benzene-thiol-ato-kappa(2) S:S)bis-(μ-phenyl-methane-thiol-ato-kappa(2) S:S)bis-[(η⁶-1-isopropyl-4-methyl-

- benzene)-ruthenium(II)] tetra-fluorido-borate, *Acta Crystallogr., Sect. E: Crystallogr. Commun.*, 71 (2015) 1174-1176. <https://doi.org/10.1107/S2056989015016953>.
- [78] F. Cherieux, C.M. Thomas, T. Monnier, G. Suss-Fink, Specific reactivity of SH versus OH functions towards dinuclear arene ruthenium units: synthesis of cationic complexes of the type [(arene)(2)Ru(2)(SR)(3)](+), *Polyhedron*, 22 (2003) 543-548. [https://doi.org/10.1016/S0277-5387\(02\)01376-1](https://doi.org/10.1016/S0277-5387(02)01376-1).
- [79] V. Studer, N. Anghel, O. Desiatkina, T. Felder, G. Boubaker, Y. Amdouni, J. Ramseier, M. Hungerbühler, C. Kempf, J.T. Heverhagen, A. Hemphill, N. Ruprecht, J. Furrer, E. Paunescu, Conjugates containing two and three trithiolato-bridged dinuclear ruthenium(II)-arene anits as in vitro antiparasitic and anticancer agents, *Pharmaceuticals*, 13 (2020). <https://doi.org/10.3390/ph13120471>.
- [80] J.R. Newcomb, B. Rivnay, C.M. Bastos, T.D. Ocain, K. Gordon, P. Gregory, S.M. Turci, K.A. Sterne, M. Jesson, J. Krieger, J.C. Jenson, B. Jones, In vitro immunomodulatory activity of ruthenium complexes, *Inflammation Res.*, 52 (2003) 263-271. <https://doi.org/10.1007/s00011-003-1169-5>.
- [81] C.M. Bastos, K.A. Gordon, T.D. Ocain, Synthesis and immunosuppressive activity of ruthenium complexes, *Bioorg. Med. Chem. Lett.*, 8 (1998) 147-150. [https://doi.org/10.1016/S0960-894X\(97\)10205-0](https://doi.org/10.1016/S0960-894X(97)10205-0).
- [82] E. Gjini, P.H. Brito, Integrating antimicrobial therapy with host immunity to fight drug-resistant infections: classical vs. adaptive treatment, *PLoS Comput. Biol.*, 12 (2016) e1004857. <https://doi.org/10.1371/journal.pcbi.1004857>.
- [83] A. Coutinho, E. Gronowicz, W.W. Bullock, G. Moller, Mechanism of thymus-independent immunocyte triggering. Mitogenic activation of B cells results in specific immune responses, *J. Exp. Med.*, 139 (1974) 74-92. <https://doi.org/10.1084/jem.139.1.74>.
- [84] R. Dziarski, Preferential induction of autoantibody secretion in polyclonal activation by peptidoglycan and lipopolysaccharide. II. In vivo studies, *J. Immunol.*, 128 (1982) 1026-1030.
- [85] R. Palacios, Concanavalin A triggers T lymphocytes by directly interacting with their receptors for activation, *J. Immunol.*, 128 (1982) 337-342.
- [86] E.D. Hawkins, M.L. Turner, C.J. Wellard, J.H. Zhou, M.R. Dowling, P.D. Hodgkin, Quantal and graded stimulation of B lymphocytes as alternative strategies for regulating adaptive immune responses, *Nat. Commun.*, 4 (2013) 2406. <https://doi.org/10.1038/ncomms3406>.
- [87] Y. Oxford Diffraction Ltd., Oxfordshire, UK., Oxford Diffraction. CrysAlisPro (Version 1.171.40.37a)., in, 2018.
- [88] P. Macchi, H.B. Burgi, A.S. Chimpri, J. Hauser, Z. Gal, Low-energy contamination of Mo microsource X-ray radiation: analysis and solution of the problem, *J. Appl. Crystallogr.*, 44 (2011) 763-771. <https://doi.org/10.1107/S0021889811016232>.
- [89] G.M. Sheldrick, SHELXT - integrated space-group and crystal-structure determination, *Acta Crystallogr., Sect. A: Found. Adv.*, 71 (2015) 3-8. <https://doi.org/10.1107/S2053273314026370>.
- [90] G.M. Sheldrick, Crystal structure refinement with SHELXL, *Acta Crystallogr., Sect. C: Struct. Chem.*, 71 (2015) 3-8. <https://doi.org/10.1107/S2053229614024218>.
- [91] O.V. Dolomanov, L.J. Bourhis, R.J. Gildea, J.A.K. Howard, H. Puschmann, OLEX2: a complete structure solution, refinement and analysis program, *J. Appl. Crystallogr.*, 42 (2009) 339-341. <https://doi.org/10.1107/S0021889808042726>.
- [92] A.L. Spek, PLATON SQUEEZE: a tool for the calculation of the disordered solvent contribution to the calculated structure factors, *Acta Crystallogr., Sect. C: Struct. Chem.*, 71 (2015) 9-18. <https://doi.org/10.1107/S2053229614024929>.
- [93] P. Winzer, J. Muller, A. Aguado-Martinez, M. Rahman, V. Balmer, V. Manser, L.M. Ortega-Mora, K.K. Ojo, E.K. Fan, D.J. Maly, W.C. Van Voorhis, A. Hemphill, In vitro and in vivo effects of the bumped kinase inhibitor 1294 in the related cyst-forming apicomplexans *Toxoplasma gondii* and *Neospora caninum*, *Antimicrob. Agents Chemother.*, 59 (2015) 6361-6374. <https://doi.org/10.1128/AAC.01236-15>.
- [94] J. Muller, A. Aguado-Martinez, V. Manser, H.N. Wong, R.K. Haynes, A. Hemphill, Repurposing of antiparasitic drugs: the hydroxy-naphthoquinone buparvaquone inhibits vertical transmission in the pregnant neosporosis mouse model, *Vet. Res.*, 47 (2016). <https://doi.org/10.1186/s13567-016-0317-1>.

- 56 compounds (54 ruthenium and 2 osmium) were synthesized and investigated.
- They are based on the trithiolato-bridged dinuclear ruthenium(II)-arene scaffold.
- The *in vitro* assessment was realized using a three-step screening cascade.
- One polar group and two CF₃ groups on the bridge thiols is the best combination.
- 1 compound exhibited the most favorable features.

Author declaration

[Instructions: Please check all applicable boxes and provide additional information as requested.]

1. Conflict of Interest

Potential conflict of interest exists:

We wish to draw the attention of the Editor to the following facts, which may be considered as potential conflicts of interest, and to significant financial contributions to this work:

The nature of potential conflict of interest is described below:

X No conflict of interest exists.

We wish to confirm that there are no known conflicts of interest associated with this publication and there has been no significant financial support for this work that could have influenced its outcome.

2. Funding

X Funding was received for this work.

All of the sources of funding for the work described in this publication are acknowledged below:

- *Swiss Science National Foundation (SNF, Sinergia project CRSII5-173718 and project no. 310030_184662).*
- *Swiss Governmental Excellence Fellowship.*
- *Swiss Science National Foundation SNF within the (R'Equip programme no. 206021_177033).*

☐ No funding was received for this work.

3. Intellectual Property

X We confirm that we have given due consideration to the protection of intellectual property associated with this work and that there are no impediments to publication, including the timing of publication, with respect to intellectual property. In so doing we confirm that we have followed the regulations of our institutions concerning intellectual property.

4. Research Ethics

☐ We further confirm that any aspect of the work covered in this manuscript that has involved human patients has been conducted with the ethical approval of all relevant bodies and that such approvals are acknowledged within the manuscript.

☐ IRB approval was obtained (required for studies and series of 3 or more cases)

☐ Written consent to publish potentially identifying information, such as details or the case and photographs, was obtained from the patient(s) or their legal guardian(s).

5. Authorship

The International Committee of Medical Journal Editors (ICMJE) recommends that authorship be based on the following four criteria:

1. Substantial contributions to the conception or design of the work; or the acquisition, analysis, or interpretation of data for the work; AND
2. Drafting the work or revising it critically for important intellectual content; AND
3. Final approval of the version to be published; AND
4. Agreement to be accountable for all aspects of the work in ensuring that questions related to the accuracy or integrity of any part of the work are appropriately investigated and resolved.

All those designated as authors should meet all four criteria for authorship, and all who meet the four criteria should be identified as authors. For more information on authorship, please see <http://www.icmje.org/recommendations/browse/roles-and-responsibilities/defining-the-role-of-authors-and-contributors.html#two>.

X All listed authors meet the ICMJE criteria. We attest that all authors contributed significantly to the creation of this manuscript, each having fulfilled criteria as established by the ICMJE.

☐ One or more listed authors do(es) not meet the ICMJE criteria.

We believe these individuals should be listed as authors because:

[Please elaborate below]

X We confirm that the manuscript has been read and approved by all named authors.

X We confirm that the order of authors listed in the manuscript has been approved by all named authors.

6. Contact with the Editorial Office

The Corresponding Author declared on the title page of the manuscript is:

[Insert name below]

X This author submitted this manuscript using his/her account in EVISE.

X We understand that this Corresponding Author is the sole contact for the Editorial process (including EVISE and direct communications with the office). He/she is responsible for communicating with the other authors about progress, submissions of revisions and final approval of proofs.

X We confirm that the email address shown below is accessible by the Corresponding Author, is the address to which Corresponding Author's EVISE account is linked, and has been configured to accept email from the editorial office of American Journal of Ophthalmology Case Reports:

julien.furrer@dcb.unibe.ch

☐ Someone other than the Corresponding Author declared above submitted this manuscript from his/her account in EVISE:

[Insert name below]

☐ We understand that this author is the sole contact for the Editorial process (including EVISE and direct communications with the office). He/she is responsible for communicating with the other authors, including the Corresponding Author, about progress, submissions of revisions and final approval of proofs.

We the undersigned agree with all of the above.

Author's name (Fist, Last)	Signature	Date
1. _Julien Furrer_	_JF_	_07/04/2021_
2. _Oksana Desiatkina_	OD	07/04/2021
3. _Emilia Păunescu	_EP_	_08/04/2021_
4. _Nicoleta Anghel_	NA	7.04.2021
5. _Ghalia Boubaker	_GB_	_07/04/2021_
6. _Andrew Hemphil_	_AH_	_07/04/2021_
7. _Yosra Amdouni_	_YA_	08.04.2021_
8. _____	_____	_____
9. _____	_____	_____
10. _____	_____	_____

Journal Pre-proof